# MAXWELL'S EQUATIONS, ELECTROMAGNETIC WAVES, AND STOKES PARAMETERS

MICHAEL I. MISHCHENKO AND LARRY D. TRAVIS

*NASA Goddard Institute for Space Studies, 2880 Broadway, New York, NY 10025, USA*

## 1. Introduction

The theoretical basis for describing elastic scattering of light by particles and surfaces is formed by classical electromagnetics. In order to make this volume sufficiently self-contained, this introductory chapter provides a summary of those concepts and equations of electromagnetic theory that will be used extensively in later chapters and introduces the necessary notation.

We start by formulating the macroscopic Maxwell equations and constitutive relations and discussing the fundamental time-harmonic plane-wave solution that underlies the basic optical idea of a monochromatic parallel beam of light. This is followed by the introduction of the Stokes parameters and a discussion of their ellipsometric content. Then we consider the concept of a quasi-monochromatic beam of light and its implications and briefly discuss how the Stokes parameters of monochromatic and quasi-monochromatic light can be measured in practice. In the final two sections, we discuss another fundamental solution of Maxwell's equations in the form of a time-harmonic outgoing spherical wave and introduce the concept of the coherency dyad, which plays a vital role in the theory of multiple light scattering by random particle ensembles.

## 2. Maxwell's equations and constitutive relations

The theory of classical optics phenomena is based on the set of four Maxwell's equations for the macroscopic electromagnetic field at interior points in matter, which in SI units read:

$$\nabla \cdot \mathcal{D}(\mathbf{r}, t) = \rho(\mathbf{r}, t), \tag{2.1}$$

$$\nabla \times \mathcal{E}(\mathbf{r}, t) = -\frac{\partial \mathcal{B}(\mathbf{r}, t)}{\partial t}, \tag{2.2}$$

$$\nabla \cdot \mathcal{B}(\mathbf{r}, t) = 0, \tag{2.3}$$



*G. Videen, Ya. Yatskiv and M. Mishchenko (eds.), Photopolarimetry in Remote Sensing,* 1–44.
2004 *Kluwer Academic Publishers. Printed in the Netherlands.*

$$\nabla \times \mathcal{H}(\mathbf{r}, t) = \mathcal{J}(\mathbf{r}, t) + \frac{\partial \mathcal{D}(\mathbf{r}, t)}{\partial t}, \tag{2.4}$$

where $\mathcal{E}$ is the electric and $\mathcal{H}$ the magnetic field, $\mathcal{B}$ the magnetic induction, $\mathcal{D}$ the electric displacement, and $\rho$ and $\mathcal{J}$ the macroscopic (free) charge density and current density, respectively. All quantities entering Eqs. (2.1)–(2.4) are functions of time, $t$, and spatial coordinates, $\mathbf{r}$. Implicit in the Maxwell equations is the continuity equation

$$\frac{\partial \rho(\mathbf{r}, t)}{\partial t} + \nabla \cdot \mathcal{J}(\mathbf{r}, t) = 0, \tag{2.5}$$

which is obtained by combining the time derivative of Eq. (2.1) with the divergence of Eq. (2.4) and taking into account that $\nabla \cdot (\nabla \times \mathbf{a}) = 0$. The vector fields entering Eqs. (2.1)–(2.4) are related by

$$\mathcal{D}(\mathbf{r}, t) = \epsilon_0 \mathcal{E}(\mathbf{r}, t) + \mathcal{P}(\mathbf{r}, t), \tag{2.6}$$

$$\mathcal{H}(\mathbf{r}, t) = \frac{1}{\mu_0} \mathcal{B}(\mathbf{r}, t) - \mathcal{M}(\mathbf{r}, t), \tag{2.7}$$

where $\mathcal{P}$ is the electric polarization (average electric dipole moment per unit volume), $\mathcal{M}$ is the magnetization (average magnetic dipole moment per unit volume), and $\epsilon_0$ and $\mu_0$ are the electric permittivity and the magnetic permeability of free space, respectively.

Equations (2.1)–(2.7) are insufficient for a unique determination of the electric and magnetic fields from a given distribution of charges and currents and must be supplemented with so-called constitutive relations:

$$\mathcal{P}(\mathbf{r}, t) = \epsilon_0 \chi(\mathbf{r}) \mathcal{E}(\mathbf{r}, t), \tag{2.8}$$

$$\mathcal{B}(\mathbf{r}, t) = \mu(\mathbf{r}) \mathcal{H}(\mathbf{r}, t), \tag{2.9}$$

$$\mathcal{J}(\mathbf{r}, t) = \sigma(\mathbf{r}) \mathcal{E}(\mathbf{r}, t), \tag{2.10}$$

where $\chi$ is the electric susceptibility, $\mu$ the magnetic permeability, and $\sigma$ the conductivity. Equations (2.6) and (2.8) yield

$$\mathcal{D}(\mathbf{r}, t) = \epsilon(\mathbf{r}) \mathcal{E}(\mathbf{r}, t), \tag{2.11}$$

where

$$\epsilon(\mathbf{r}) = \epsilon_0 [1 + \chi(\mathbf{r})] \tag{2.12}$$

is the electric permittivity. For linear and isotropic media, $\chi$, $\mu$, $\sigma$, and $\epsilon$ are scalars independent of the fields. The microphysical derivation and the range of validity of the macroscopic Maxwell equations are discussed in detail by Jackson [1].

The constitutive relations (2.9)–(2.11) connect the field vectors at the same moment of time $t$ and are valid for electromagnetic fields in a vacuum and also for electromagnetic fields in macroscopic material media provided that the

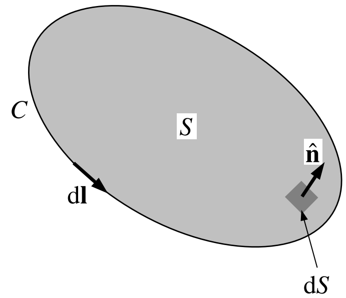


Figure 2.1: A finite surface $S$ bounded by a closed contour $C$.

fields are constant or vary in time rather slowly. For a rapidly varying field in a material medium, the state of the medium depends not only on the current value of the field but also on the values of the field at all previous times. Therefore, for a linear, time-invariant medium, the constitutive relations (2.9)–(2.11) must be replaced by the following general causal relations that take into account the effect of the prior history on the electromagnetic properties of the medium:

$$\mathcal{D}(\mathbf{r},t) = \int_{-\infty}^{t} \mathrm{d}t' \tilde{\epsilon}(\mathbf{r}, t-t')\mathcal{E}(\mathbf{r},t'), \tag{2.13}$$

$$\mathcal{B}(\mathbf{r},t) = \int_{-\infty}^{t} \mathrm{d}t' \tilde{\mu}(\mathbf{r}, t-t')\mathcal{H}(\mathbf{r},t'), \tag{2.14}$$

$$\mathcal{J}(\mathbf{r},t) = \int_{-\infty}^{t} \mathrm{d}t' \tilde{\sigma}(\mathbf{r}, t-t')\mathcal{E}(\mathbf{r},t'). \tag{2.15}$$

The medium characterized by the constitutive relations (2.13)–(2.15) is called time-dispersive.

It is straightforward to rewrite the Maxwell equations and the continuity equation in an integral form. Specifically, integrating Eqs. (2.2) and (2.4) over a surface $S$ bounded by a closed contour $C$ (see Fig. 2.1) and applying the Stokes theorem,

$$\int_S \mathrm{d}S(\nabla\times\mathbf{A})\cdot\hat{\mathbf{n}} = \oint_C \mathrm{d}\mathbf{l}\cdot\mathbf{A}, \tag{2.16}$$

yield

$$\oint_C \mathrm{d}\mathbf{l}\cdot\mathcal{E} = -\frac{\partial}{\partial t}\int_S \mathrm{d}S\mathcal{B}\cdot\hat{\mathbf{n}}, \tag{2.17}$$

$$\oint_C \mathrm{d}\mathbf{l}\cdot\mathcal{H} = \int_S \mathrm{d}S\mathcal{J}\cdot\hat{\mathbf{n}} + \frac{\partial}{\partial t}\int_S \mathrm{d}S\mathcal{D}\cdot\hat{\mathbf{n}}, \tag{2.18}$$

where we employ the usual convention that the direction of the differential

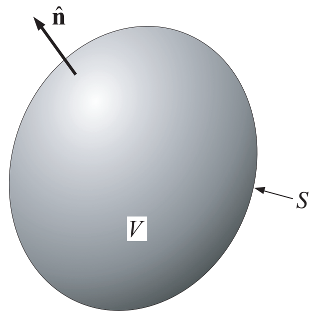


Figure 2.2: A finite volume $V$ bounded by a closed surface $S$.

length vector $\mathrm{d}\mathbf{l}$ is related to the direction of the unit vector along the local normal to the surface $\hat{\mathbf{n}}$ according to the right-hand rule.

Similarly, integrating Eqs. (2.1), (2.3), and (2.5) over a finite volume $V$ bounded by a closed surface $S$ (see Fig. 2.2) and using the Gauss theorem,

$$\int_V \mathrm{d}\mathbf{r}\nabla\cdot\mathbf{A} = \oint_S \mathrm{d}S\mathbf{A}\cdot\hat{\mathbf{n}}, \tag{2.19}$$

we derive

$$\oint_S \mathrm{d}S\boldsymbol{\mathcal{D}}\cdot\hat{\mathbf{n}} = \int_V \mathrm{d}\mathbf{r}\rho, \tag{2.20}$$

$$\oint_S \mathrm{d}S\boldsymbol{\mathcal{B}}\cdot\hat{\mathbf{n}} = 0, \tag{2.21}$$

$$\oint_S \mathrm{d}S\boldsymbol{\mathcal{J}}\cdot\hat{\mathbf{n}} = -\frac{\partial}{\partial t}\int_V \mathrm{d}\mathbf{r}\rho, \tag{2.22}$$

where the unit vector $\hat{\mathbf{n}}$ is directed along the outward local normal to the surface.

## 3. Boundary conditions

The Maxwell equations are strictly valid only for points in whose neighborhood the physical properties of the medium, as characterized by the constitutive parameters $\chi$, $\mu$, and, $\sigma$ vary continuously. However, across an interface separating one medium from another the constitutive parameters may change abruptly, and one may expect similar discontinuous behavior of the field vectors $\boldsymbol{\mathcal{E}}$, $\boldsymbol{\mathcal{D}}$, $\boldsymbol{\mathcal{B}}$, and $\boldsymbol{\mathcal{H}}$. The boundary conditions at such an interface can be derived from the integral form of the Maxwell equations as follows. Consider two different continuous media separated by an interface $S$ as shown in Fig. 3.1. Let $\hat{\mathbf{n}}$ be a unit vector along the local normal to the interface, pointing from medium 1 toward medium 2. Let us take the integral in Eq.

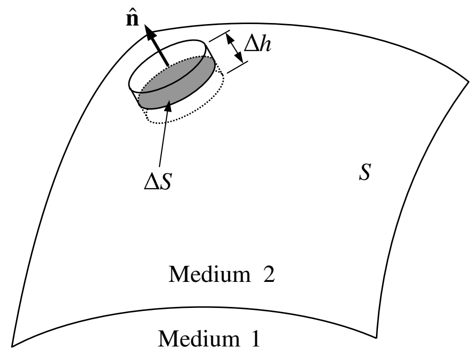


Figure 3.1: Pillbox used in the derivation of boundary conditions for the $\mathcal{B}$ and $\mathcal{D}$.

(2.21) over the closed surface of a small cylinder with bases parallel to a small surface element $\Delta S$ such that half of the cylinder is in medium 1 and half in medium 2. The contribution from the curved surface of the cylinder vanishes in the limit $\Delta h \to 0$, and we thus obtain

$$(\mathcal{B}_2 - \mathcal{B}_1)\cdot\hat{\mathbf{n}} = 0, \tag{3.1}$$

which means that the normal component of the magnetic induction is continuous across the interface.

Similarly, evaluating the integrals on the left- and right-hand sides of Eq. (2.20) over the surface and volume of the cylinder, respectively, we derive

$$(\mathcal{D}_2 - \mathcal{D}_1)\cdot\hat{\mathbf{n}} = \lim_{\Delta h\to 0}\Delta h\rho = \rho_S, \tag{3.2}$$

where $\rho_S$ is the surface charge density (charge per unit area) measured in coulombs per square meter. Thus, there is a discontinuity in the normal component of $\mathcal{D}$ if the interface carries a layer of surface charge density.

Let us now consider a small rectangular loop of area $\Delta A$ formed by sides of length $\Delta l$ perpendicular to the local normal and ends of length $\Delta h$ parallel to the local normal, as shown in Fig. 3.2. The surface integral on the right-hand side of Eq. (2.17) vanishes in the limit $\Delta h \to 0$,

$$\lim_{\Delta h\to 0}\int_{\Delta A}\mathrm{d}S\mathcal{B}\cdot(\hat{\mathbf{n}}\times\hat{\mathbf{l}}) = \lim_{\Delta h\to 0}\Delta l\Delta h\mathcal{B}\cdot(\hat{\mathbf{n}}\times\hat{\mathbf{l}}) = 0,$$

so that

$$\hat{\mathbf{l}}\cdot(\mathcal{E}_2 - \mathcal{E}_1) = 0. \tag{3.3}$$

Since the orientation of the rectangle – and hence also of $\hat{\mathbf{l}}$ – is arbitrary, Eq. (3.3) means that the vector $\mathcal{E}_2 - \mathcal{E}_1$ must be perpendicular to the interface. Thus,

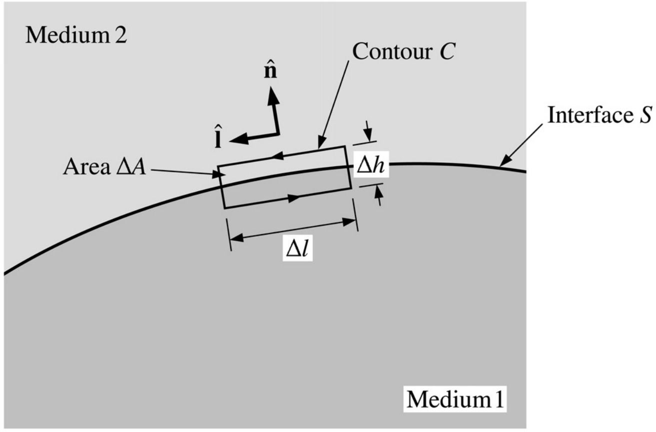


Figure 3.2: Rectangular loop used in the derivation of boundary conditions for the $\mathcal{E}$ and $\mathcal{H}$.

$$\hat{\mathbf{n}}\times(\mathcal{E}_2 - \mathcal{E}_1) = \mathbf{0}, \tag{3.4}$$

where $\mathbf{0}$ is a zero vector. This implies that the tangential component of $\mathcal{E}$ is continuous across the interface.

Similarly, Eq. (2.18) yields

$$\hat{\mathbf{l}}\cdot(\mathcal{H}_2 - \mathcal{H}_1) = \lim_{\Delta h\to 0} \Delta h(\hat{\mathbf{n}}\times\hat{\mathbf{l}})\cdot\mathcal{J} = (\hat{\mathbf{n}}\times\hat{\mathbf{l}})\cdot\mathcal{J}_S, \tag{3.5}$$

where $\mathcal{J}_S$ is the surface current density measured in amperes per meter. Since

$$\hat{\mathbf{l}} = (\hat{\mathbf{n}}\times\hat{\mathbf{l}})\times\hat{\mathbf{n}}, \tag{3.6}$$

we can use the vector identity

$$(\mathbf{a}\times\mathbf{b})\cdot\mathbf{c} = \mathbf{a}\cdot(\mathbf{b}\times\mathbf{c}) \tag{3.7}$$

to derive

$$[(\hat{\mathbf{n}}\times\hat{\mathbf{l}})\times\hat{\mathbf{n}}]\cdot(\mathcal{H}_2 - \mathcal{H}_1) = (\hat{\mathbf{n}}\times\hat{\mathbf{l}})\cdot[\hat{\mathbf{n}}\times(\mathcal{H}_2 - \mathcal{H}_1)] = (\hat{\mathbf{n}}\times\hat{\mathbf{l}})\cdot\mathcal{J}_S. \tag{3.8}$$

Since this equality must be valid for any orientation of the rectangle and, thus, of the tangent unit vector $\hat{\mathbf{l}}$, we finally have

$$\hat{\mathbf{n}}\times(\mathcal{H}_2 - \mathcal{H}_1) = \mathcal{J}_S, \tag{3.9}$$

which means that there is a discontinuity in the tangential component of $\mathcal{H}$ if the interface can carry a surface current. Media with finite conductivity cannot support surface currents so that

$$\hat{\mathbf{n}} \times (\mathcal{H}_2 - \mathcal{H}_1) = \mathbf{0} \qquad \text{(finite conductivity).} \tag{3.10}$$

The boundary conditions (3.1), (3.2), (3.4), (3.9), and (3.10) are useful in solving the differential Maxwell equations in different adjacent regions with continuous physical properties and then linking the partial solutions to determine the fields throughout all space.

## 4. Time-harmonic fields

Let us now assume that all fields and sources are time harmonic (or monochromatic), which means that their time dependence can be fully described by expressing them as sums of terms proportional to either $\cos\omega t$ or $\sin\omega t$, where $\omega$ is the angular frequency. It is standard practice to represent real monochromatic fields as real parts of the respective complex time-harmonic fields, e.g.,

$$\begin{aligned} \mathcal{E}(\mathbf{r},t) &= \mathrm{Re}\,\mathbf{E}(\mathbf{r},t) = \mathrm{Re}[\mathbf{E}(\mathbf{r})\exp(-\mathrm{i}\omega t)] \\ &= \tfrac{1}{2}[\mathbf{E}(\mathbf{r})\exp(-\mathrm{i}\omega t) + \mathbf{E}^*(\mathbf{r})\exp(\mathrm{i}\omega t)] \end{aligned} \tag{4.1}$$

and analogously for $\mathcal{D}$, $\mathcal{H}$, $\mathcal{B}$, $\mathcal{J}$, $\rho$, $\mathcal{P}$, and $\mathcal{M}$, where $\mathrm{i} = \sqrt{-1}$, $\mathbf{E}(\mathbf{r})$ is complex, and the asterisk denotes a complex-conjugate value. Equations (2.1)–(2.5) then yield the following frequency-domain Maxwell equations and continuity equation for the time-independent components of the complex fields:

$$\nabla \cdot \mathbf{D}(\mathbf{r}) = \rho(\mathbf{r}), \tag{4.2}$$

$$\nabla \times \mathbf{E}(\mathbf{r}) = \mathrm{i}\omega\mathbf{B}(\mathbf{r}), \tag{4.3}$$

$$\nabla \cdot \mathbf{B}(\mathbf{r}) = 0, \tag{4.4}$$

$$\nabla \times \mathbf{H}(\mathbf{r}) = \mathbf{J}(\mathbf{r}) - \mathrm{i}\omega\mathbf{D}(\mathbf{r}), \tag{4.5}$$

$$-\mathrm{i}\omega\rho(\mathbf{r}) + \nabla \cdot \mathbf{J}(\mathbf{r}) = 0, \tag{4.6}$$

where we emphasize the typographical distinction between the real quantities $\mathcal{E}$, $\mathcal{D}$, $\mathcal{H}$, $\mathcal{B}$, $\mathcal{J}$, and $\rho$ and their complex counterparts $\mathbf{E}$, $\mathbf{D}$, $\mathbf{H}$, $\mathbf{B}$, $\mathbf{J}$, and $\mathrm{\rho}$.

The constitutive relations remain unchanged in the frequency domain for a non-dispersive medium:

$$\mathbf{D}(\mathbf{r}) = \epsilon(\mathbf{r})\mathbf{E}(\mathbf{r}), \tag{4.7}$$

$$\mathbf{B}(\mathbf{r}) = \mu(\mathbf{r})\mathbf{H}(\mathbf{r}), \tag{4.8}$$

$$\mathbf{J}(\mathbf{r}) = \sigma(\mathbf{r})\mathbf{E}(\mathbf{r}). \tag{4.9}$$

For a time-dispersive medium, we can substitute the monochromatic fields of the form (4.1) into Eqs. (2.13)–(2.15), which yields

$$\mathbf{D}(\mathbf{r}) = \mathrm{\epsilon}(\mathbf{r},\omega)\mathbf{E}(\mathbf{r}), \tag{4.10}$$

$$\mathbf{B}(\mathbf{r}) = \mathrm{\mu}(\mathbf{r},\omega)\mathbf{H}(\mathbf{r}), \tag{4.11}$$

$$\mathbf{J}(\mathbf{r}) = \mathrm{\sigma}(\mathbf{r},\omega)\mathbf{E}(\mathbf{r}), \tag{4.12}$$

where

$$\epsilon(\mathbf{r},\omega) = \int_0^\infty \mathrm{d}t\,\tilde{\epsilon}(\mathbf{r},t)\exp(\mathrm{i}\omega t), \tag{4.13}$$

$$\mu(\mathbf{r},\omega) = \int_0^\infty \mathrm{d}t\,\tilde{\mu}(\mathbf{r},t)\exp(\mathrm{i}\omega t), \tag{4.14}$$

$$\sigma(\mathbf{r},\omega) = \int_0^\infty \mathrm{d}t\,\tilde{\sigma}(\mathbf{r},t)\exp(\mathrm{i}\omega t) \tag{4.15}$$

are complex functions of the angular frequency. Note that we use sloping Greek letters in Eqs. (4.7)–(4.9) and upright Greek letters in Eqs. (4.10)–(4.12) to differentiate between the frequency-independent and the frequency-dependent constitutive parameters, respectively. Equations (4.2) and (4.5) can be rewritten in the form

$$\nabla\cdot[\varepsilon(\mathbf{r},\omega)\mathbf{E}(\mathbf{r})] = 0, \tag{4.16}$$

$$\nabla\times\mathbf{H}(\mathbf{r}) = -\mathrm{i}\omega\varepsilon(\mathbf{r},\omega)\mathbf{E}(\mathbf{r}), \tag{4.17}$$

where

$$\varepsilon(\mathbf{r},\omega) = \epsilon(\mathbf{r},\omega) + \mathrm{i}\frac{\sigma(\mathbf{r},\omega)}{\omega} \tag{4.18}$$

is the so-called complex permittivity. Again, the reader should note the typographical distinction between the frequency-dependent electric permittivity $\epsilon$ (which can, in principle, be complex-valued for a dispersive medium) and the complex permittivity $\varepsilon$. We will show later that a direct consequence of a complex-valued $\varepsilon$ and/or $\mu$ is a non-zero imaginary part of the refractive index (Eq. (6.19)), which causes absorption of electromagnetic energy (Eq. (6.20)) by converting it into other forms of energy, e.g., heat.

The scalar or the vector product of two real vector fields is not equal to the real part of the respective product of the corresponding complex vector fields. Instead,

$$\begin{aligned}\mathcal{c}(\mathbf{r},t) &= \boldsymbol{\mathcal{a}}(\mathbf{r},t)\cdot\boldsymbol{\mathcal{b}}(\mathbf{r},t)\\ &= \tfrac{1}{4}[\mathbf{a}(\mathbf{r})\exp(-\mathrm{i}\omega t) + \mathbf{a}^*(\mathbf{r})\exp(\mathrm{i}\omega t)]\\ &\quad\cdot[\mathbf{b}(\mathbf{r})\exp(-\mathrm{i}\omega t) + \mathbf{b}^*(\mathbf{r})\exp(\mathrm{i}\omega t)]\\ &= \tfrac{1}{2}\mathrm{Re}[\mathbf{a}(\mathbf{r})\cdot\mathbf{b}^*(\mathbf{r}) + \mathbf{a}(\mathbf{r})\cdot\mathbf{b}(\mathbf{r})\exp(-2\mathrm{i}\omega t)],\end{aligned} \tag{4.19}$$

and similarly for a vector product. Usually the angular frequency $\omega$ is so high that traditional optical measuring devices are not capable of following the rapid oscillations of the instantaneous product values but rather respond to a time average

$$\langle \mathcal{c}(\mathbf{r},t)\rangle_t = \frac{1}{T}\int_t^{t+T}\mathrm{d}\tau\,\mathcal{c}(\mathbf{r},\tau), \tag{4.20}$$

where $T$ is a time interval long compared with $1/\omega$. Therefore, Eqs. (4.19) and (4.20) imply that the time average of a product of two real fields is equal to one half of the real part of the respective product of one complex field with the complex conjugate of the other, e.g.,

$$\langle c(\mathbf{r},t)\rangle_t = \tfrac{1}{2}\mathrm{Re}[\mathbf{a}(\mathbf{r})\cdot\mathbf{b}^*(\mathbf{r})]. \tag{4.21}$$

## 5. The Poynting vector

Both the value and the direction of the electromagnetic energy flow are described by the so-called Poynting vector $\mathcal{S}$. The expression for $\mathcal{S}$ can be derived by considering conservation of energy and taking into account that the magnetic field does no work and that for a local charge $q$ the rate of doing work by the electric field is $q(\mathbf{r},t)\mathbf{v}(\mathbf{r},t)\cdot\mathcal{E}(\mathbf{r},t)$, where $\mathbf{v}$ is the velocity of the charge. Indeed, the total rate of doing work by the electromagnetic field in a finite volume $V$ is given by

$$\int_V \mathrm{d}\mathbf{r}\,\mathcal{J}(\mathbf{r},t)\cdot\mathcal{E}(\mathbf{r},t) \tag{5.1}$$

and represents the rate of conversion of electromagnetic energy into mechanical or thermal energy. This power must be balanced by the corresponding rate of decrease of the electromagnetic field energy within the volume $V$. Using Eqs. (2.2) and (2.4) and the vector identity

$$\nabla\cdot(\mathbf{a}\times\mathbf{b}) = \mathbf{b}\cdot(\nabla\times\mathbf{a}) - \mathbf{a}\cdot(\nabla\times\mathbf{b}), \tag{5.2}$$

we derive

$$\begin{aligned}\int_V \mathrm{d}\mathbf{r}\,\mathcal{J}\cdot\mathcal{E} &= \int_V \mathrm{d}\mathbf{r}\,\mathcal{E}\cdot\left(\nabla\times\mathcal{H} - \frac{\partial\mathcal{D}}{\partial t}\right)\\ &= -\int_V \mathrm{d}\mathbf{r}\left[\nabla\cdot(\mathcal{E}\times\mathcal{H}) + \mathcal{E}\cdot\frac{\partial\mathcal{D}}{\partial t} + \mathcal{H}\cdot\frac{\partial\mathcal{B}}{\partial t}\right].\end{aligned} \tag{5.3}$$

Let us first consider a linear medium without dispersion and introduce the total electromagnetic energy density,

$$u(\mathbf{r},t) = \tfrac{1}{2}[\mathcal{E}(\mathbf{r},t)\cdot\mathcal{D}(\mathbf{r},t) + \mathcal{B}(\mathbf{r},t)\cdot\mathcal{H}(\mathbf{r},t)], \tag{5.4}$$

and the so-called Poynting vector,

$$\mathcal{S}(\mathbf{r},t) = \mathcal{E}(\mathbf{r},t)\times\mathcal{H}(\mathbf{r},t). \tag{5.5}$$

The latter represents electromagnetic energy flow and has the dimension [energy/(area × time)]. Using also the Gauss theorem (2.19), we finally obtain

$$\int_V \mathrm{d}\mathbf{r}\,\mathcal{J}\cdot\mathcal{E} + \int_V \mathrm{d}\mathbf{r}\frac{\partial u}{\partial t} + \oint_S \mathrm{d}S\,\mathcal{S}\cdot\hat{\mathbf{n}} = 0, \tag{5.6}$$

where the closed surface $S$ bounds the volume $V$ and $\hat{\mathbf{n}}$ is a unit vector in the direction of the local outward normal to the surface. Equation (5.6) manifests the conservation of energy by requiring that the rate of the total work done by the fields on the sources within the volume, the time rate of change of electromagnetic energy within the volume, and the electromagnetic energy flowing out through the volume boundary per unit time add up to zero. Since the volume $V$ is arbitrary, Eq. (5.3) also can be written in the form of a differential continuity equation:

$$\frac{\partial u}{\partial t} + \nabla \cdot \mathcal{S} = -\mathcal{J} \cdot \mathcal{E}. \tag{5.7}$$

Since $\nabla \cdot (\nabla \times \mathbf{a}) = 0$, it is clear from Eq. (5.7) that adding the curl of a vector field to the Poynting vector will not change the energy balance, which seems to suggest that there is a degree of arbitrariness in the definition of the Poynting vector. However, relativistic considerations discussed in section 12.10 of Jackson [1] show that the definition (5.5) is, in fact, unique.

Let us now allow the medium to be dispersive. Instead of Eq. (5.1), we now consider the integral

$$\frac{1}{2} \int_V \mathrm{d}\mathbf{r} \mathbf{J}^*(\mathbf{r}) \cdot \mathbf{E}(\mathbf{r}) \tag{5.8}$$

whose real part gives the time-averaged rate of work done by the electromagnetic field (cf. Eq. (4.21)). Using Eqs. (4.3), (4.5), and (5.2), we derive

$$\begin{aligned} \frac{1}{2} \int_V \mathrm{d}\mathbf{r} \mathbf{J}^*(\mathbf{r}) \cdot \mathbf{E}(\mathbf{r}) &= \frac{1}{2} \int_V \mathrm{d}\mathbf{r} \mathbf{E}(\mathbf{r}) \cdot [\nabla \times \mathbf{H}^*(\mathbf{r}) - \mathrm{i}\omega \mathbf{D}^*(\mathbf{r})] \\ &= -\frac{1}{2} \int_V \mathrm{d}\mathbf{r} \{\nabla \cdot [\mathbf{E}(\mathbf{r}) \times \mathbf{H}^*(\mathbf{r})] \\ &\qquad + \mathrm{i}\omega [\mathbf{E}(\mathbf{r}) \cdot \mathbf{D}^*(\mathbf{r}) - \mathbf{B}(\mathbf{r}) \cdot \mathbf{H}^*(\mathbf{r})]\}. \end{aligned} \tag{5.9}$$

If we now define the complex Poynting vector by

$$\mathbf{S}(\mathbf{r}) = \tfrac{1}{2}[\mathbf{E}(\mathbf{r}) \times \mathbf{H}^*(\mathbf{r})] \tag{5.10}$$

and the complex electric and magnetic energy densities by

$$w_e(\mathbf{r}) = \tfrac{1}{4}[\mathbf{E}(\mathbf{r}) \cdot \mathbf{D}^*(\mathbf{r})], \tag{5.11}$$

$$w_m(\mathbf{r}) = \tfrac{1}{4}[\mathbf{B}(\mathbf{r}) \cdot \mathbf{H}^*(\mathbf{r})], \tag{5.12}$$

respectively, and apply the Gauss theorem, we then have

$$\frac{1}{2} \int_V \mathrm{d}\mathbf{r} \mathbf{J}^*(\mathbf{r}) \cdot \mathbf{E}(\mathbf{r}) + \oint_S \mathrm{d}S \mathbf{S}(\mathbf{r}) \cdot \hat{\mathbf{n}} + 2\mathrm{i}\omega \int_V \mathrm{d}\mathbf{r} [w_e(\mathbf{r}) - w_m(\mathbf{r})] = 0. \tag{5.13}$$

Obviously, the real part of Eq. (5.13) manifests the conservation of energy for the corresponding time-averaged quantities. In particular, the time-averaged Poynting vector $\langle \mathcal{S}(\mathbf{r},t)\rangle_t$ is equal to the real part of the complex Poynting vector,

$$\langle \mathcal{S}(\mathbf{r},t)\rangle_t = \mathrm{Re}[\mathbf{S}(\mathbf{r})]. \tag{5.14}$$

The net rate $W$ at which the electromagnetic energy crosses the surface $S$ is given by

$$W = -\oint_S \mathrm{d}S \langle \mathcal{S}(\mathbf{r},t)\rangle_t \cdot \hat{\mathbf{n}}. \tag{5.15}$$

The rate is defined such that it is positive if there is a net transfer of electromagnetic energy into the volume $V$ and is negative otherwise.

## 6. Plane-wave solution

Consider an infinite homogeneous medium. The use of the formulas

$$\nabla\cdot(f\mathbf{a}) = f\,\nabla\cdot\mathbf{a} + (\nabla f)\cdot\mathbf{a}, \tag{6.1}$$

$$\nabla\times(f\mathbf{a}) = f\,\nabla\times\mathbf{a} + (\nabla f)\times\mathbf{a}, \tag{6.2}$$

$$\nabla\exp(\mathrm{i}\mathbf{k}\cdot\mathbf{r}) = \mathrm{i}\mathbf{k}\exp(\mathrm{i}\mathbf{k}\cdot\mathbf{r}) \tag{6.3}$$

in Eqs. (4.3), (4.4), (4.16), and (4.17) shows that the complex field vectors

$$\mathbf{E}(\mathbf{r},t) = \mathbf{E}_0\exp(\mathrm{i}\mathbf{k}\cdot\mathbf{r}-\mathrm{i}\omega t), \tag{6.4}$$

$$\mathbf{H}(\mathbf{r},t) = \mathbf{H}_0\exp(\mathrm{i}\mathbf{k}\cdot\mathbf{r}-\mathrm{i}\omega t), \tag{6.5}$$

where $\mathbf{E}_0$, $\mathbf{H}_0$, and $\mathbf{k}$ are constant complex vectors, are a solution of the Maxwell equations provided that

$$\mathbf{k}\cdot\mathbf{E}_0 = 0, \tag{6.6}$$

$$\mathbf{k}\cdot\mathbf{H}_0 = 0, \tag{6.7}$$

$$\mathbf{k}\times\mathbf{E}_0 = \omega\mu\mathbf{H}_0, \tag{6.8}$$

$$\mathbf{k}\times\mathbf{H}_0 = -\omega\varepsilon\mathbf{E}_0. \tag{6.9}$$

The so-called wave vector $\mathbf{k}$ is usually expressed as

$$\mathbf{k} = \mathbf{k}_\mathrm{R} + \mathrm{i}\mathbf{k}_\mathrm{I}, \tag{6.10}$$

where $\mathbf{k}_\mathrm{R}$ and $\mathbf{k}_\mathrm{I}$ are real vectors. Thus

$$\mathbf{E}(\mathbf{r},t) = \mathbf{E}_0\exp(-\mathbf{k}_\mathrm{I}\cdot\mathbf{r})\exp(\mathrm{i}\mathbf{k}_\mathrm{R}\cdot\mathbf{r}-\mathrm{i}\omega t), \tag{6.11}$$

$$\mathbf{H}(\mathbf{r},t) = \mathbf{H}_0\exp(-\mathbf{k}_\mathrm{I}\cdot\mathbf{r})\exp(\mathrm{i}\mathbf{k}_\mathrm{R}\cdot\mathbf{r}-\mathrm{i}\omega t). \tag{6.12}$$

The $\mathbf{E}_0\exp(-\mathbf{k}_\mathrm{I}\cdot\mathbf{r})$ and $\mathbf{H}_0\exp(-\mathbf{k}_\mathrm{I}\cdot\mathbf{r})$ are the complex amplitudes of the electric and magnetic fields, respectively, and $\phi = \mathbf{k}_\mathrm{R}\cdot\mathbf{r}-\omega t$ is their phase.

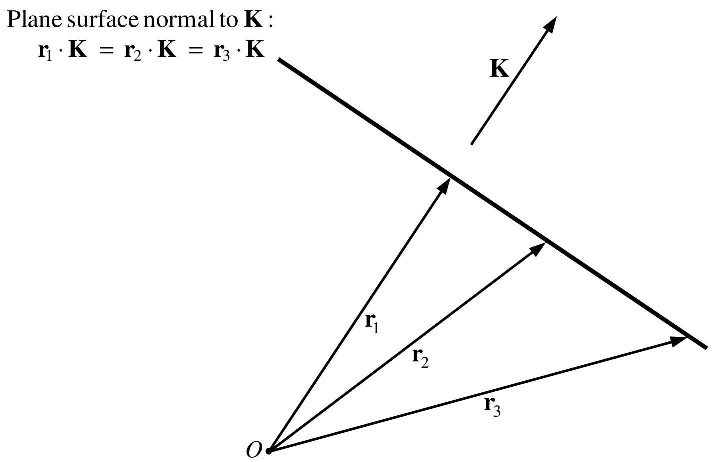


Figure 6.1: Plane surface normal to a real vector $\mathbf{K}$.

The vector $\mathbf{k}_{\mathrm{R}}$ is normal to the surfaces of constant phase, whereas $\mathbf{k}_{\mathrm{I}}$ is normal to the surfaces of constant amplitude. Indeed, a plane surface normal to a real vector $\mathbf{K}$ is described by $\mathbf{r}\cdot\mathbf{K} = \text{constant}$, where $\mathbf{r}$ is the radius vector drawn from the origin of the reference frame to any point in the plane (see Fig.

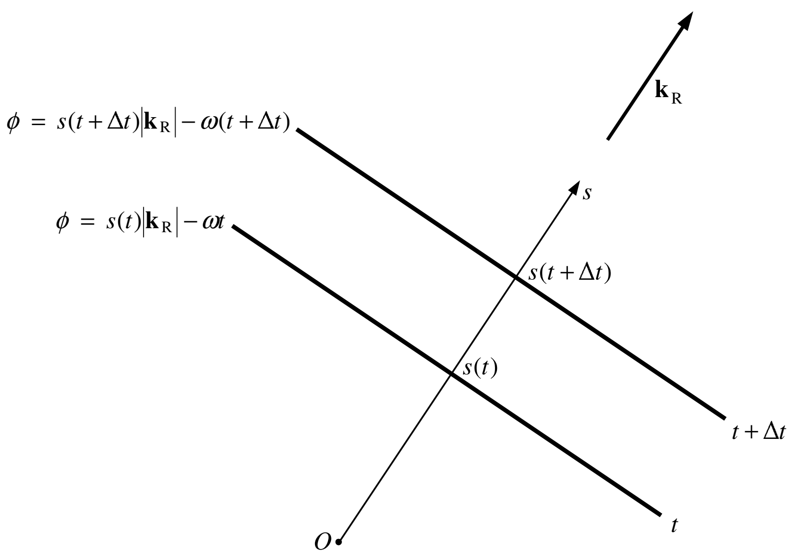


Figure 6.2: The plane of constant phase $\phi = \text{constant}$ travels a distance $\Delta s$ over the time period $\Delta t$ . The $s$-axis is drawn from the origin of the coordinate system along the vector $\mathbf{k}_{\mathrm{R}}$.

6.1). Also, it is easy to see that surfaces of constant phase propagate in the direction of $\mathbf{k}_R$ with the phase velocity

$$v = \omega / |\mathbf{k}_R|. \tag{6.13}$$

Indeed, the planes corresponding to the instantaneous times $t$ and $t + \Delta t$ are separated by the distance $\Delta s = \omega \Delta t / |\mathbf{k}_R|$ (see Fig. 6.2), which gives Eq. (6.13). Thus Eqs. (6.4) and (6.5) describe a plane electromagnetic wave propagating in a homogeneous medium without sources. This is a very important solution of the Maxwell equations because it embodies the concept of a perfectly monochromatic parallel beam of light of infinite lateral extent and represents the transport of electromagnetic energy from one point to another.

Equations (6.4) and (6.8) yield

$$\mathbf{H}(\mathbf{r}, t) = \frac{1}{\omega \mu} \mathbf{k} \times \mathbf{E}(\mathbf{r}, t). \tag{6.14}$$

Therefore, a plane electromagnetic wave always can be considered in terms of only the electric (or only the magnetic) field.

The electromagnetic wave is called homogeneous if $\mathbf{k}_R$ and $\mathbf{k}_I$ are parallel (including the case $\mathbf{k}_I = \mathbf{0}$); otherwise it is called inhomogeneous. When $\mathbf{k}_R \parallel \mathbf{k}_I$, the complex wave vector can be expressed as $\mathbf{k} = (k_R + \mathrm{i}k_I)\hat{\mathbf{n}}$, where $\hat{\mathbf{n}}$ is a real unit vector in the direction of propagation and both $k_R$ and $k_I$ are real and nonnegative.

According to Eqs. (6.6) and (6.7), the plane electromagnetic wave is transverse: both $\mathbf{E}_0$ and $\mathbf{H}_0$ are perpendicular to $\mathbf{k}$. Furthermore, it is evident from either Eq. (6.8) or Eq. (6.9) that $\mathbf{E}_0$ and $\mathbf{H}_0$ are mutually perpendicular: $\mathbf{E}_0 \cdot \mathbf{H}_0 = 0$. Since $\mathbf{E}_0$, $\mathbf{H}_0$, and $\mathbf{k}$ are, in general, complex vectors, the physical interpretation of these facts can be far from obvious. It becomes most transparent when both $\varepsilon$, $\mu$, and $\mathbf{k}$ are real. The reader can easily verify that in this case the real field vectors $\mathcal{E}$ and $\mathcal{H}$ are mutually perpendicular and lie in a plane normal to the direction of wave propagation $\hat{\mathbf{n}}$ (see Fig. 6.3).

Taking the vector product of $\mathbf{k}$ with the left-hand side and the right-hand side of Eq. (6.8) and using Eq. (6.9) and the vector identity

$$\mathbf{a} \times (\mathbf{b} \times \mathbf{c}) = \mathbf{b}(\mathbf{a} \cdot \mathbf{c}) - \mathbf{c}(\mathbf{a} \cdot \mathbf{b}) \tag{6.15}$$

together with Eq. (6.6) yield

$$\mathbf{k} \cdot \mathbf{k} = \omega^2 \varepsilon \mu. \tag{6.16}$$

In the practically important case of a homogeneous plane wave, we obtain from Eq. (6.16)

$$k = k_R + \mathrm{i}k_I = \omega \sqrt{\varepsilon \mu} = \frac{\omega m}{c}, \tag{6.17}$$

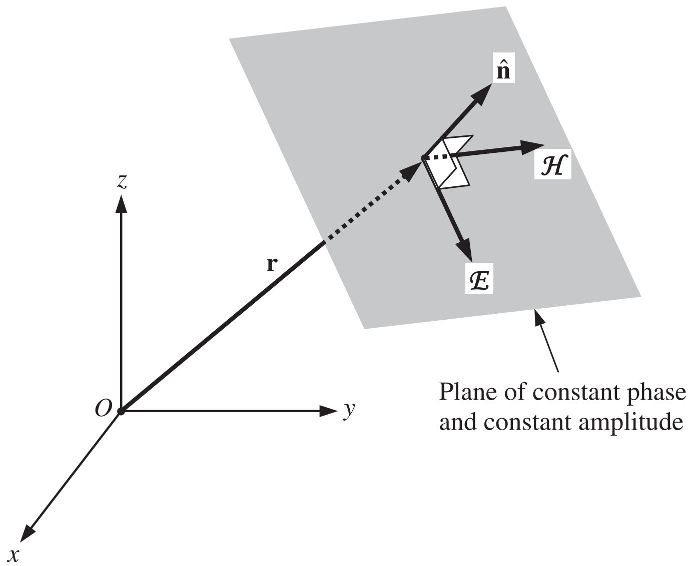


Figure 6.3: Plane wave propagating in a homogeneous medium with no dispersion and losses.

where $k$ is the wave number,

$$c = \frac{1}{\sqrt{\epsilon_0 \mu_0}} \tag{6.18}$$

is the speed of light in a vacuum (cf. Eq. (6.13)), and

$$m = \frac{ck}{\omega} = m_{\mathrm{R}} + \mathrm{i}m_{\mathrm{I}} = \sqrt{\frac{\varepsilon\mu}{\epsilon_0 \mu_0}} = c\sqrt{\varepsilon\mu} \tag{6.19}$$

is the complex refractive index with a non-negative real part $m_{\mathrm{R}}$ and a non-negative imaginary part $m_{\mathrm{I}}$. Thus, the complex electric field vector of the homogeneous plane wave has the form

$$\mathbf{E}(\mathbf{r}, t) = \mathbf{E}_0 \exp\left(-\frac{\omega}{c} m_{\mathrm{I}} \hat{\mathbf{n}} \cdot \mathbf{r}\right) \exp\left(\mathrm{i}\frac{\omega}{c} m_{\mathrm{R}} \hat{\mathbf{n}} \cdot \mathbf{r} - \mathrm{i}\omega t\right). \tag{6.20}$$

If the imaginary part of the refractive index is non-zero, then it determines the decay of the amplitude of the wave as it propagates through the medium, which is thus absorbing. On the other hand, a medium is nonabsorbing if it is non-dispersive ($\varepsilon = \epsilon$ and $\mu = \mu$) and lossless ($\sigma = 0$), which causes the refractive index $m = m_{\mathrm{R}} = c\sqrt{\epsilon\mu}$ to be real-valued. The real part of the refractive index determines the phase velocity of the wave:

$$v = \frac{c}{m_R}. \tag{6.21}$$

In a vacuum, $m = m_R = 1$ and $v = c$.

As follows from Eqs. (5.10), (5.14), (6.4), (6.5), (6.8), and (6.15), the time-averaged Poynting vector of a plane wave is

$$\langle \mathcal{S}(\mathbf{r}, t)\rangle_t = \mathrm{Re}\left(\frac{\mathbf{k}^*[\mathbf{E}(\mathbf{r})\cdot\mathbf{E}^*(\mathbf{r})] - \mathbf{E}^*(\mathbf{r})[\mathbf{k}^*\cdot\mathbf{E}(\mathbf{r})]}{2\omega\mu^*}\right). \tag{6.22}$$

If the wave is homogeneous, $\mathbf{k}\cdot\mathbf{E}(\mathbf{r}) = 0$ causes $\mathbf{k}^*\cdot\mathbf{E}(\mathbf{r}) = 0$. Therefore,

$$\langle \mathcal{S}(\mathbf{r}, t)\rangle_t = \tfrac{1}{2}\mathrm{Re}\left(\sqrt{\frac{\varepsilon}{\mu}}\right)|\mathbf{E}_0|^2 \exp\left(-2\frac{\omega}{c}m_I\hat{\mathbf{n}}\cdot\mathbf{r}\right)\hat{\mathbf{n}}. \tag{6.23}$$

Thus, $\langle \mathcal{S}(\mathbf{r}, t)\rangle_t$ is in the direction of propagation and its absolute value, called intensity, is attenuated exponentially provided that the medium is absorbing:

$$I(\mathbf{r}) = |\langle \mathcal{S}(\mathbf{r}, t)\rangle_t| = I_0\exp(-\alpha\hat{\mathbf{n}}\cdot\mathbf{r}), \tag{6.24}$$

where $I_0$ is the intensity at $\mathbf{r} = \mathbf{0}$. The absorption coefficient $\alpha$ is

$$\alpha = 2\frac{\omega}{c}m_I = \frac{4\pi m_I}{\lambda_0}, \tag{6.25}$$

where

$$\lambda_0 = \frac{2\pi c}{\omega} \tag{6.26}$$

is the free-space wavelength. The intensity has the dimension of monochromatic energy flux, [energy/(area × time)], and is equal to the amount of electromagnetic energy crossing a unit surface element normal to $\hat{\mathbf{n}}$ per unit time.

The expression for the time-averaged energy density of a plane wave propagating in a medium without dispersion follows from Eqs. (4.7), (4.8), (4.21) and (5.4):

$$\langle u(\mathbf{r}, t)\rangle_t = \tfrac{1}{4}[\epsilon\mathbf{E}(\mathbf{r})\cdot\mathbf{E}^*(\mathbf{r}) + \mu\mathbf{H}(\mathbf{r})\cdot\mathbf{H}^*(\mathbf{r})]. \tag{6.27}$$

Assuming further that the medium is lossless and recalling Eqs. (4.3), (6.8) and (6.16) and the vector identity

$$(\mathbf{a}\times\mathbf{b})\cdot(\mathbf{c}\times\mathbf{d}) = (\mathbf{a}\cdot\mathbf{c})(\mathbf{b}\cdot\mathbf{d}) - (\mathbf{a}\cdot\mathbf{d})(\mathbf{b}\cdot\mathbf{c}), \tag{6.28}$$

we derive

$$\langle u(\mathbf{r}, t)\rangle_t = \tfrac{1}{2}\epsilon|\mathbf{E}_0|^2. \tag{6.29}$$

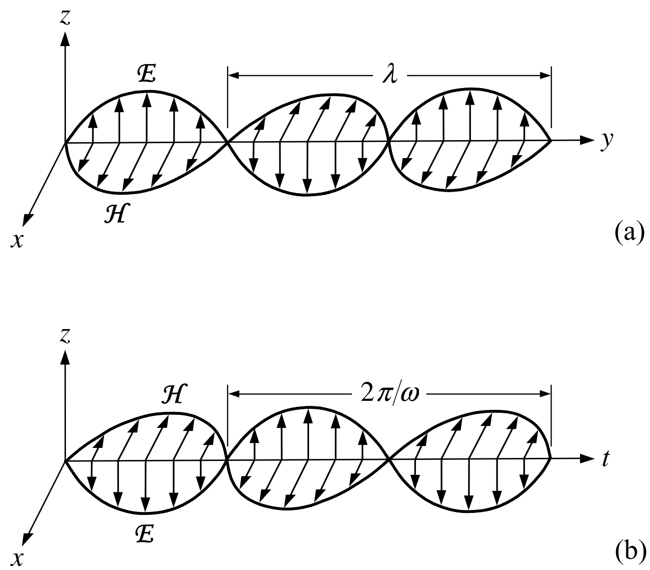


Figure 6.4: Plane electromagnetic wave described by Eqs. (6.31) and (6.32).

Comparison of Eqs. (6.23), (6.24), and (6.29) yields

$$I(\mathbf{r}) = \frac{1}{\sqrt{\epsilon\mu}} \langle u(\mathbf{r},t)\rangle_t = v\langle u(\mathbf{r},t)\rangle_t, \tag{6.30}$$

where $v$ is the speed of light in the nonabsorbing material medium. The physical interpretation of this result is quite clear: the amount of electromagnetic energy crossing a surface element of unit area normal to the direction of propagation per unit time is equal to the product of the speed of light and the amount of electromagnetic energy per unit volume.

Figure 6.4 gives a simple example of a plane electromagnetic wave propagating in a nonabsorbing homogeneous medium and described by the following real electric and magnetic field vectors:

$$\mathcal{E}(\mathbf{r},t) = \mathcal{E}\cos(ky - \omega t - \pi/2)\,\hat{\mathbf{z}}, \tag{6.31}$$

$$\mathcal{H}(\mathbf{r},t) = \mathcal{H}\cos(ky - \omega t - \pi/2)\,\hat{\mathbf{x}}, \tag{6.32}$$

where $\mathcal{E}$, $\mathcal{H}$, and $k$ are real and $\hat{\mathbf{x}}$ and $\hat{\mathbf{z}}$ are the unit vectors along the $x$-axis and the $z$-axis, respectively. Panel (a) shows the electric and magnetic fields as a function of $y$ at the moment $t = 0$, while panel (b) depicts the fields as a function of time at any point in the plane $y = 0$. The period of the sinusoids in panel (a) is given by

$$\lambda = \frac{2\pi}{k} \tag{6.33}$$

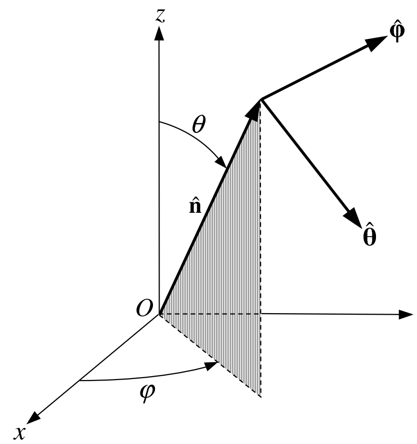


Figure 7.1: Local coordinate system used to describe the direction of propagation and polarization state of a plane electromagnetic wave at the observation point *O*.

and defines the wavelength of light in the nonabsorbing material medium, whereas the period of the sinusoids in panel (b) is equal to $2\pi/\omega$.

It is straightforward to verify that the choice of the $\exp(\mathrm{i}\omega t)$ rather than $\exp(-\mathrm{i}\omega t)$ time dependence in the complex representation of time-harmonic fields in Eq. (4.1) would have led to $m = m_R - \mathrm{i}m_I$ with a non-negative $m_I$. The $\exp(-\mathrm{i}\omega t)$ time factor convention adopted here was used in many books on optics and light scattering (e.g., [2–6]), electromagnetics (e.g., [1,7–9]), and solid-state physics. On the other hand, van de Hulst [10], Kerker [11], and Hovenier and van der Mee [12] use the time factor $\exp(\mathrm{i}\omega t)$, which implies a non-positive imaginary part of the complex refractive index. It does not matter in the final analysis which convention is chosen because all measurable quantities of practical interest are always real. However, it is important to remember that once a choice of the time factor has been made, its consistent use throughout all derivations is imperative.

## 7. Coherency matrix and Stokes parameters

Traditional optical devices cannot measure the electric and magnetic fields associated with a beam of light but rather measure quantities that are time averages of real-valued linear combinations of products of field vector components and have the dimension of the intensity. In order to define these quantities, we use polar spherical coordinates associated with the local right-handed Cartesian coordinate system with origin at the observation point, as shown in Fig. 7.1. Assuming that the medium is homogeneous and has no dispersion and losses, we specify the direction of propagation of a plane electromagnetic wave by a unit vector $\hat{\mathbf{n}}$ or, equivalently, by a couple $\{\theta, \varphi\}$, where $\theta \in [0, \pi]$ is the polar (zenith) angle measured from the positive $z$-axis and $\varphi \in [0, 2\pi)$ is the azimuth angle measured from the positive $x$-axis in the clockwise direction when looking in the direction of the positive $z$-axis. Since the component of the electric field vector along the direction of propagation $\hat{\mathbf{n}}$ is equal to zero, the electric field at the observation point can be expressed as $\mathbf{E} = \mathbf{E}_\theta + \mathbf{E}_\varphi$, where $\mathbf{E}_\theta$ and $\mathbf{E}_\varphi$ are the $\theta$- and $\varphi$-components of the electric field vector, respectively. The component $\mathbf{E}_\theta = E_\theta \hat{\boldsymbol{\theta}}$ lies in the meridional plane (i.e., the plane through $\hat{\mathbf{n}}$ and the $z$-axis), whereas the component $\mathbf{E}_\varphi = E_\varphi \hat{\boldsymbol{\varphi}}$ is perpendicular to this plane. $\hat{\boldsymbol{\theta}}$ and $\hat{\boldsymbol{\varphi}}$ are the corresponding unit vectors such that $\hat{\mathbf{n}} = \hat{\boldsymbol{\theta}} \times \hat{\boldsymbol{\varphi}}$.

The specification of a unit vector $\hat{\mathbf{n}}$ uniquely determines the meridional plane of the propagation direction except when $\hat{\mathbf{n}}$ is oriented along the positive or negative direction of the $z$ axis. Although it may seem redundant to specify $\varphi$ in addition to $\theta$ when $\theta = 0$ or $\pi$, the unit $\hat{\boldsymbol{\theta}}$ and $\hat{\boldsymbol{\varphi}}$ vectors and, thus, the electric field vector components $\mathbf{E}_\theta$ and $\mathbf{E}_\varphi$ still depend on the orientation of the meridional plane. Therefore, we always assume that the specification of $\hat{\mathbf{n}}$ implicitly includes the specification of the appropriate meridional plane in cases when $\hat{\mathbf{n}}$ is parallel to the $z$ axis.

Consider a plane electromagnetic wave propagating in a homogeneous medium without dispersion and losses and given by

$$\mathbf{E}(\mathbf{r},t) = \mathbf{E}_0 \exp(\mathrm{i}k\hat{\mathbf{n}} \cdot \mathbf{r} - \mathrm{i}\omega t) \tag{7.1}$$

with a real $k$. The simplest complete set of linearly independent quadratic combinations of the electric field vector components with non-zero time averages consists of the following four quantities:

$$E_\theta(\mathbf{r},t)E_\theta^*(\mathbf{r},t) = E_{0\theta}E_{0\theta}^*, \qquad E_\theta(\mathbf{r},t)E_\varphi^*(\mathbf{r},t) = E_{0\theta}E_{0\varphi}^*,$$
$$E_\varphi(\mathbf{r},t)E_\theta^*(\mathbf{r},t) = E_{0\varphi}E_{0\theta}^*, \qquad E_\varphi(\mathbf{r},t)E_\varphi^*(\mathbf{r},t) = E_{0\varphi}E_{0\varphi}^*.$$

The products of these quantities and $\frac{1}{2}\sqrt{\epsilon/\mu}$ have the dimension of monochromatic energy flux and form the $2\times 2$ coherency (or density) matrix $\boldsymbol{\rho}$ [2]:

$$\boldsymbol{\rho} = \begin{bmatrix} \rho_{11} & \rho_{12} \\ \rho_{21} & \rho_{22} \end{bmatrix} = \frac{1}{2}\sqrt{\frac{\epsilon}{\mu}} \begin{bmatrix} E_{0\theta}E_{0\theta}^* & E_{0\theta}E_{0\varphi}^* \\ E_{0\varphi}E_{0\theta}^* & E_{0\varphi}E_{0\varphi}^* \end{bmatrix}. \tag{7.2}$$

The completeness of the set of the four coherency matrix elements means that any plane wave characteristic directly observable with a traditional optical instrument is a real-valued linear combination of these quantities.

Since $\rho_{12}$ and $\rho_{21}$ are, in general, complex, it is convenient to introduce an alternative complete set of four real, linearly independent quantities called Stokes parameters [13]. We first group the elements of the $2\times 2$ coherency matrix into a $4\times 1$ coherency column vector:

$$\mathbf{J} = \begin{bmatrix} \rho_{11} \\ \rho_{12} \\ \rho_{21} \\ \rho_{22} \end{bmatrix} = \frac{1}{2}\sqrt{\frac{\epsilon}{\mu}} \begin{bmatrix} E_{0\theta}E_{0\theta}^* \\ E_{0\theta}E_{0\varphi}^* \\ E_{0\varphi}E_{0\theta}^* \\ E_{0\varphi}E_{0\varphi}^* \end{bmatrix}. \tag{7.3}$$

The Stokes parameters $I$, $Q$, $U$, and $V$ are then defined as the elements of a $4\times 1$ column Stokes vector $\mathbf{I}$ as follows:

$$\mathbf{I} = \begin{bmatrix} I \\ Q \\ U \\ V \end{bmatrix} = \mathbf{DJ} = \frac{1}{2}\sqrt{\frac{\epsilon}{\mu}} \begin{bmatrix} E_{0\theta}E_{0\theta}^* + E_{0\varphi}E_{0\varphi}^* \\ E_{0\theta}E_{0\theta}^* - E_{0\varphi}E_{0\varphi}^* \\ -E_{0\theta}E_{0\varphi}^* - E_{0\varphi}E_{0\theta}^* \\ \mathrm{i}(E_{0\varphi}E_{0\theta}^* - E_{0\theta}E_{0\varphi}^*) \end{bmatrix}, \tag{7.4}$$

where

$$\mathbf{D} = \begin{bmatrix} 1 & 0 & 0 & 1 \\ 1 & 0 & 0 & -1 \\ 0 & -1 & -1 & 0 \\ 0 & -\mathrm{i} & \mathrm{i} & 0 \end{bmatrix}. \tag{7.5}$$

Conversely,

$$\mathbf{J} = \mathbf{D}^{-1}\mathbf{I}, \tag{7.6}$$

where

$$\mathbf{D}^{-1} = \frac{1}{2}\begin{bmatrix} 1 & 1 & 0 & 0 \\ 0 & 0 & -1 & \mathrm{i} \\ 0 & 0 & -1 & -\mathrm{i} \\ 1 & -1 & 0 & 0 \end{bmatrix}. \tag{7.7}$$

By virtue of being real-valued quantities and having the dimension of energy flux, the Stokes parameters form a complete set of quantities that are needed to characterize a plane electromagnetic wave, inasmuch as it is subject to practical analysis. This means that (i) any other observable quantity is a linear combination of the four Stokes parameters, and (ii) it is impossible to distinguish between two plane waves with the same values of the Stokes parameters using a traditional optical device (the so-called principle of optical equivalence). Indeed, the two complex amplitudes $E_{0\theta} = a_\theta \exp(\mathrm{i}\Delta_\theta)$ and $E_{0\varphi} = a_\varphi \exp(\mathrm{i}\Delta_\varphi)$ are characterized by four real numbers: the non-negative amplitudes $a_\theta$ and $a_\varphi$ and the phases $\Delta_\theta$ and $\Delta_\varphi = \Delta_\theta - \Delta$. The Stokes parameters carry information about the amplitudes and the phase difference $\Delta$, but not about $\Delta_\theta$. The latter is the only quantity that could be used to distinguish different waves with the same $a_\theta$, $a_\varphi$, and $\Delta$ (and thus the same Stokes parameters), but it vanishes when a field vector component is multiplied by the complex conjugate value of the same or another field vector component.

The first Stokes parameter, $I$, is the intensity introduced in the previous section, with the explicit definition here applicable to a homogeneous, nonabsorbing medium. The Stokes parameters $Q$, $U$, and $V$ describe the polarization state of the wave. The ellipsometric interpretation of the Stokes parameters will be the subject of the next section. It is easy to verify that the Stokes parameters of a plane monochromatic wave are not completely independent but rather are related by the quadratic identity

$$I^2 = Q^2 + U^2 + V^2. \tag{7.8}$$

We will see later, however, that this identity may not hold for a quasi-monochromatic beam of light.

The coherency matrix and the Stokes vector are not the only representations of polarization and not always the most convenient ones. Two other frequently used representations are the real so-called modified Stokes column vector given by

$$\mathbf{I}^{\mathrm{MS}} = \begin{bmatrix} I_{\mathrm{v}} \\ I_{\mathrm{h}} \\ U \\ V \end{bmatrix} = \mathbf{BI} = \begin{bmatrix} \frac{1}{2}(I + Q) \\ \frac{1}{2}(I - Q) \\ U \\ V \end{bmatrix} \tag{7.9}$$

and the complex circular-polarization column vector defined as

$$\mathbf{I}^{\mathrm{CP}} = \begin{bmatrix} I_2 \\ I_0 \\ I_{-0} \\ I_{-2} \end{bmatrix} = \mathbf{AI} = \frac{1}{2}\begin{bmatrix} Q + \mathrm{i}U \\ I + V \\ I - V \\ Q - \mathrm{i}U \end{bmatrix}, \tag{7.10}$$

where

$$\mathbf{B} = \begin{bmatrix} 1/2 & 1/2 & 0 & 0 \\ 1/2 & -1/2 & 0 & 0 \\ 0 & 0 & 1 & 0 \\ 0 & 0 & 0 & 1 \end{bmatrix}, \tag{7.11}$$

$$\mathbf{A} = \frac{1}{2}\begin{bmatrix} 0 & 1 & \mathrm{i} & 0 \\ 1 & 0 & 0 & 1 \\ 1 & 0 & 0 & -1 \\ 0 & 1 & -\mathrm{i} & 0 \end{bmatrix}. \tag{7.12}$$

It is easy to verify that

$$\mathbf{I} = \mathbf{B}^{-1}\mathbf{I}^{\mathrm{MS}} \tag{7.13}$$

and

$$\mathbf{I} = \mathbf{A}^{-1}\mathbf{I}^{\mathrm{CP}}, \tag{7.14}$$

where

$$\mathbf{B}^{-1} = \begin{bmatrix} 1 & 1 & 0 & 0 \\ 1 & -1 & 0 & 0 \\ 0 & 0 & 1 & 0 \\ 0 & 0 & 0 & 1 \end{bmatrix} \tag{7.15}$$

and

$$\mathbf{A}^{-1} = \begin{bmatrix} 0 & 1 & 1 & 0 \\ 1 & 0 & 0 & 1 \\ -\mathrm{i} & 0 & 0 & \mathrm{i} \\ 0 & 1 & -1 & 0 \end{bmatrix}. \tag{7.16}$$

The usefulness of the modified and circular-polarization Stokes vectors will be illustrated in the following section.

We conclude this section with a caution. It is important to remember that whereas the Poynting vector can be defined for an arbitrary electromagnetic field, the Stokes parameters can only be defined for transverse fields such as plane waves discussed in the previous section or spherical waves discussed in Section 12. Quite often the electromagnetic field at an observation point is not a well-defined transverse electromagnetic wave, in which case the Stokes vector formalism cannot be applied directly.

## 8. Ellipsometric interpretation of the Stokes parameters

In this section we show how the Stokes parameters can be used to derive the ellipsometric characteristics of the plane electromagnetic wave given by Eq. (7.1). Writing

$$E_{0\theta} = a_\theta \exp(\mathrm{i}\Delta_\theta), \tag{8.1}$$

$$E_{0\varphi} = a_\varphi \exp(\mathrm{i}\Delta_\varphi) \tag{8.2}$$

with real nonnegative amplitudes $a_\theta$ and $a_\varphi$ and real phases $\Delta_\theta$ and $\Delta_\varphi$ and recalling the definition (7.4), we obtain for the Stokes parameters

$$I = \frac{1}{2}\sqrt{\frac{\epsilon}{\mu}}\,(a_\theta^2 + a_\varphi^2), \tag{8.3}$$

$$Q = \frac{1}{2}\sqrt{\frac{\epsilon}{\mu}}\,(a_\theta^2 - a_\varphi^2), \tag{8.4}$$

$$U = -\sqrt{\frac{\epsilon}{\mu}}\, a_\theta a_\varphi \cos\Delta, \tag{8.5}$$

$$V = \sqrt{\frac{\epsilon}{\mu}}\, a_\theta a_\varphi \sin\Delta, \tag{8.6}$$

where

$$\Delta = \Delta_\theta - \Delta_\varphi. \tag{8.7}$$

Substituting Eqs. (8.1) and (8.2) into Eq. (7.1), we have for the real electric vector

$$\mathcal{E}_\theta(\mathbf{r},t) = a_\theta \cos(\delta_\theta - \omega t), \tag{8.8}$$

$$\mathcal{E}_\varphi(\mathbf{r},t) = a_\varphi \cos(\delta_\varphi - \omega t), \tag{8.9}$$

where

$$\delta_\theta = \Delta_\theta + k\hat{\mathbf{n}}\cdot\mathbf{r}, \tag{8.10}$$

$$\delta_\varphi = \Delta_\varphi + k\hat{\mathbf{n}}\cdot\mathbf{r}. \tag{8.11}$$

At any fixed point $O$ in space, the endpoint of the real electric vector given by Eqs. (8.8)–(8.11) describes an ellipse with specific major and minor axes and orientation (see the top panel of Fig. 8.1). The major axis of the ellipse makes an angle $\zeta$ with the positive direction of the $\varphi$-axis such that $\zeta \in [0,\pi)$. By definition, this orientation angle is obtained by rotating the $\varphi$-axis in the *clockwise* direction when looking in the direction of propagation, until it is directed along the major axis of the ellipse. The ellipticity is defined as the ratio of the minor to the major axes of the ellipse and is usually expressed as $|\tan\beta|$, where $\beta \in [-\pi/4, \pi/4]$. By definition, $\beta$ is positive when the real electric vector at $O$ rotates clockwise, as viewed by an observer looking in the direction of propagation (Fig. 8.1(a)). The polarization for positive $\beta$ is called right-handed, as opposed to the left-handed polarization corresponding to the anti-clockwise rotation of the electric vector.

To express the orientation $\zeta$ of the ellipse and the ellipticity $|\tan\beta|$ in terms of the Stokes parameters, we first write the equations representing the rotation of the real electric vector at $O$ in the form

$$\mathcal{E}_q(\mathbf{r},t) = a\sin\beta\sin(\delta - \omega t), \tag{8.12}$$

$$\mathcal{E}_p(\mathbf{r},t) = a\cos\beta\cos(\delta - \omega t), \tag{8.13}$$

where $\mathcal{E}_p$ and $\mathcal{E}_q$ are the electric field components along the major and minor axes of the ellipse, respectively (Fig. 8.1). One easily verifies that a positive (negative) $\beta$ indeed corresponds to the right-handed (left-handed) polarization. The connection between Eqs. (8.8)–(8.11) and Eqs. (8.12)–(8.13) can be established by using the simple transformation rule for rotation of a two-dimensional coordinate system:

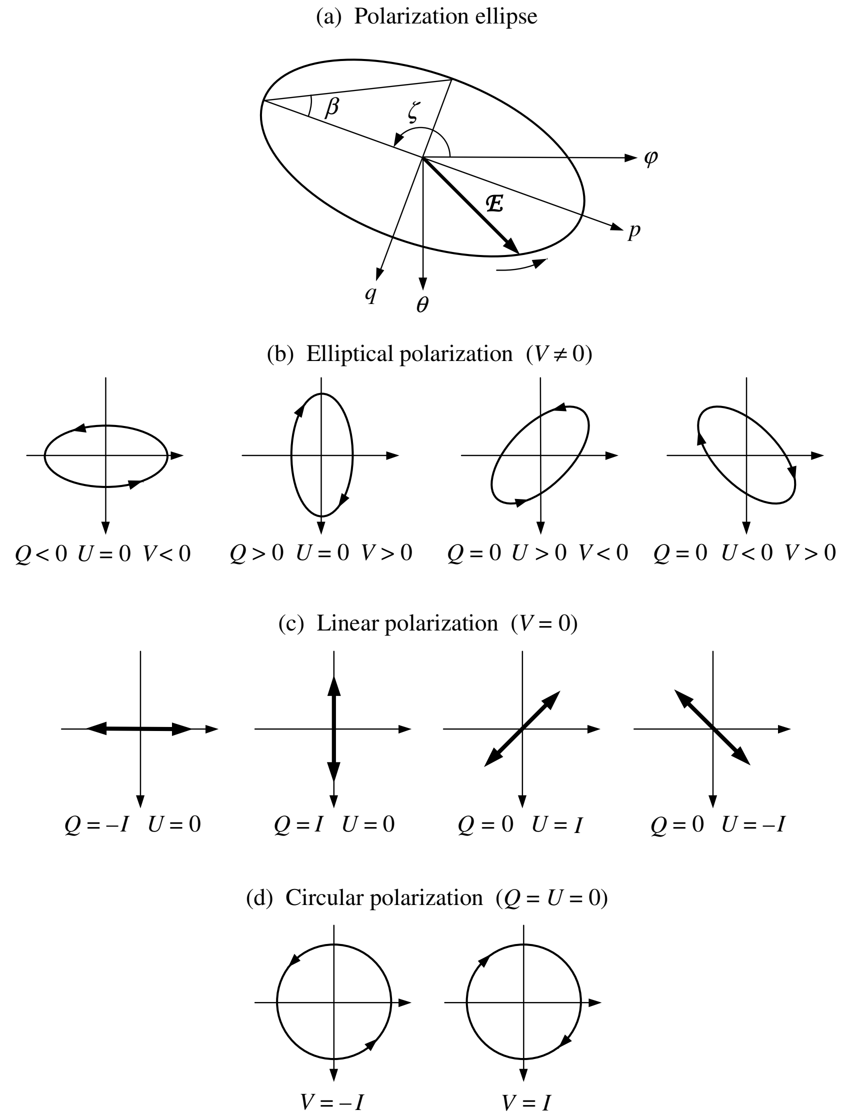


Figure 8.1: Ellipse described by the tip of the real electric vector at a fixed point $O$ in space (top panel) and particular cases of elliptical, linear, and circular polarization. The plane electromagnetic wave propagates in the direction $\hat{\boldsymbol{\theta}} \times \hat{\boldsymbol{\varphi}}$ (i.e., towards the reader).

$$\mathcal{E}_\theta(\mathbf{r},t) = -\mathcal{E}_q(\mathbf{r},t)\cos\zeta + \mathcal{E}_p(\mathbf{r},t)\sin\zeta, \tag{8.14}$$

$$\mathcal{E}_\varphi(\mathbf{r},t) = -\mathcal{E}_q(\mathbf{r},t)\sin\zeta - \mathcal{E}_p(\mathbf{r},t)\cos\zeta. \tag{8.15}$$

By equating the coefficients of $\cos\omega t$ and $\sin\omega t$ in the expanded Eqs. (8.8) and (8.9) with those in (8.14) and (8.15), we obtain

$$a_\theta \cos\delta_\theta = -a\sin\beta\sin\delta\cos\zeta + a\cos\beta\cos\delta\sin\zeta, \tag{8.16}$$
$$a_\theta \sin\delta_\theta = a\sin\beta\cos\delta\cos\zeta + a\cos\beta\sin\delta\sin\zeta, \tag{8.17}$$
$$a_\varphi \cos\delta_\varphi = -a\sin\beta\sin\delta\sin\zeta - a\cos\beta\cos\delta\cos\zeta, \tag{8.18}$$
$$a_\varphi \sin\delta_\varphi = a\sin\beta\cos\delta\sin\zeta - a\cos\beta\sin\delta\cos\zeta. \tag{8.19}$$

Squaring and adding Eqs. (8.16) and (8.17) and Eqs. (8.18) and (8.19) gives

$$a_\theta^2 = a^2(\sin^2\beta\cos^2\zeta + \cos^2\beta\sin^2\zeta), \tag{8.20}$$
$$a_\varphi^2 = a^2(\sin^2\beta\sin^2\zeta + \cos^2\beta\cos^2\zeta). \tag{8.21}$$

Multiplying Eqs. (8.16) and (8.18) and Eqs. (8.17) and (8.19) and adding yields

$$a_\theta a_\varphi \cos\Delta = -\tfrac{1}{2}a^2\cos 2\beta\sin 2\zeta. \tag{8.22}$$

Similarly, multiplying Eqs. (8.17) and (8.18) and Eqs. (8.16) and (8.19) and subtracting gives

$$a_\theta a_\varphi \sin\Delta = -\tfrac{1}{2}a^2\sin 2\beta. \tag{8.23}$$

Comparing Eqs. (8.3)–(8.6) with Eqs. (8.20)–(8.23), we finally derive

$$I = \frac{1}{2}\sqrt{\frac{\epsilon}{\mu}}\,a^2, \tag{8.24}$$
$$Q = -I\cos 2\beta\cos 2\zeta, \tag{8.25}$$
$$U = I\cos 2\beta\sin 2\zeta, \tag{8.26}$$
$$V = -I\sin 2\beta. \tag{8.27}$$

The parameters of the polarization ellipse are thus expressed in terms of the Stokes parameters as follows. The major and minor axes are given by $\sqrt{2I\sqrt{\mu/\epsilon}}\cos\beta$ and $\sqrt{2I\sqrt{\mu/\epsilon}}\,|\sin\beta|$, respectively (cf. Eqs. (8.12) and (8.13)). Equations (8.25) and (8.26) yield

$$\tan 2\zeta = -\frac{U}{Q}. \tag{8.28}$$

Because $|\beta| \le \pi/4$, we have $\cos 2\beta \ge 0$ so that $\cos 2\zeta$ has the same sign as $-Q$. Therefore, from the different values of $\zeta$ that satisfy Eq. (8.28) but differ by $\pi/2$, we must choose the one that makes the sign of $\cos 2\zeta$ to be the same as that of $-Q$. The ellipticity and handedness follow from

$$\tan 2\beta = -\frac{V}{\sqrt{Q^2+U^2}}. \tag{8.29}$$

Thus, the polarization is left-handed if $V$ is positive and is right-handed if $V$ is negative (Fig. 8.1(b)).

The electromagnetic wave is linearly polarized when $\beta = 0$; then the electric vector vibrates along the line making the angle $\zeta$ with the $\varphi$-axis (cf. Fig. 8.1) and $V = 0$. Furthermore, if $\zeta = 0$ or $\zeta = \pi/2$ then $U$ vanishes as well. This explains the usefulness of the modified Stokes representation of polarization given by Eq. (7.9) in situations involving linearly polarized light as follows. The modified Stokes vector has only one non-zero element and is equal to $[I\ 0\ 0\ 0]^{\mathrm{T}}$ if $\zeta = \pi/2$ (the electric vector vibrates along the $\theta$-axis, i.e., in the meridional plane) or $[0\ I\ 0\ 0]^{\mathrm{T}}$ if $\zeta = 0$ (the electric vector vibrates along the $\varphi$-axis, i.e., in the plane perpendicular to the meridional plane), where T indicates the transpose of a matrix (see Fig. 8.1(c)).

If, however, $\beta = \pm\pi/4$, then both $Q$ and $U$ vanish, and the electric vector describes a circle in the clockwise ($\beta = \pi/4$, $V = -I$) or anti-clockwise ($\beta = -\pi/4$, $V = I$) direction, as viewed by an observer looking in the direction of propagation (Fig. 8.1(d)). In this case the electromagnetic wave is circularly polarized; the circular-polarization vector $\mathbf{I}^{\mathrm{CP}}$ has only one non-zero element and takes the values $[0\ 0\ I\ 0]^{\mathrm{T}}$ and $[0\ I\ 0\ 0]^{\mathrm{T}}$, respectively (see Eq. (7.10)).

The polarization ellipse along with a designation of the rotation direction (right- or left-handed) fully describes the temporal evolution of the real electric vector at a fixed point in space. This evolution can also be visualized by plotting the curve in $(\theta, \varphi, t)$ coordinates described by the tip of the electric vector as a function of time. For example, in the case of an elliptically polarized plane wave with right-handed polarization, the curve is a right-handed helix with an elliptical projection onto the $\theta\varphi$-plane centered around the $t$-axis (cf. Fig. 8.2(a)). The pitch of the helix is simply $2\pi/\omega$, where $\omega$ is the angular frequency of the wave. Another way to visualize a plane wave is to fix a moment in time and draw a three-dimensional curve in $(\theta, \varphi, s)$ coordinates described by the tip of the electric vector as a function of a spatial coordinate $s = \hat{\mathbf{n}} \cdot \mathbf{r}$ oriented along the direction of propagation $\hat{\mathbf{n}}$. According to Eqs. (8.8)–(8.11), the electric field is the same for all position-time combinations with constant $ks - \omega t$. Therefore, at any instant of time (say, $t = 0$) the locus of the points described by the tip of the electric vector originating at different points on the $s$ axis is also a helix with the same projection onto the $\theta\varphi$-plane as the respective helix in the $(\theta, \varphi, t)$ coordinates, but with opposite handedness. For example, for the wave with right-handed elliptical polarization shown in Fig. 8.2(a), the respective curve in the $(\theta, \varphi, s)$ coordinates is a left-handed elliptical helix shown in Fig. 8.2(b). The pitch of this helix is the wavelength $\lambda$. It is now clear that the propagation of the wave in time and space can be represented by progressive movement in time of the helix shown in Fig. 8.2(b) in the direction of $\hat{\mathbf{n}}$ with the speed of light. With

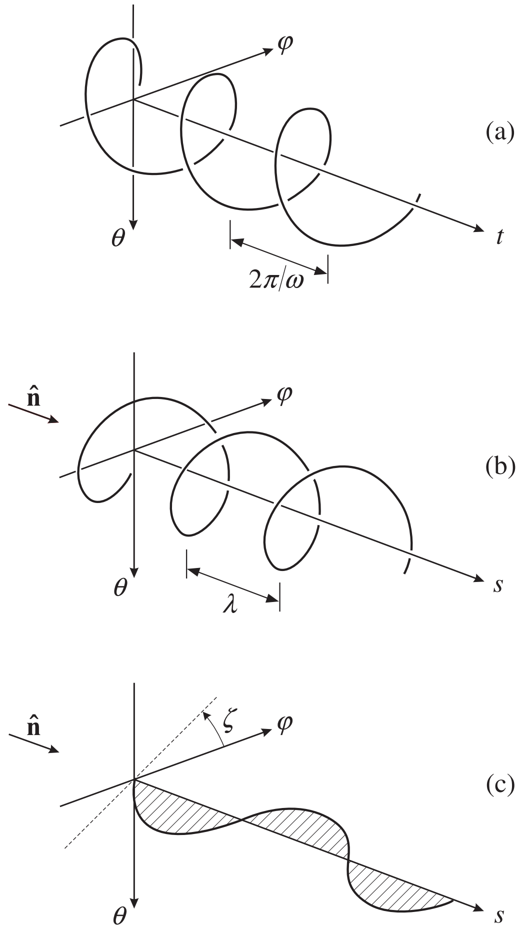


Figure 8.2: (a) The helix described by the tip of the real electric vector of a plane electromagnetic wave with right-handed polarization in $(\theta, \varphi, t)$ coordinates at a fixed point in space. (b) As in (a), but in $(\theta, \varphi, s)$ coordinates at a fixed moment in time. (c) As in (b), but for a linearly polarized wave.

increasing time, the intersection of the helix with any plane $s$ = constant describes a right-handed vibration ellipse. In the case of a circularly polarized wave, the elliptical helix becomes a helix with a circular projection onto the $\theta\varphi$-plane. If the wave is linearly polarized, then the helix degenerates into a simple sinusoidal curve in the plane making the angle $\zeta$ with the $\varphi$-axis (Fig. 8.2(c)).

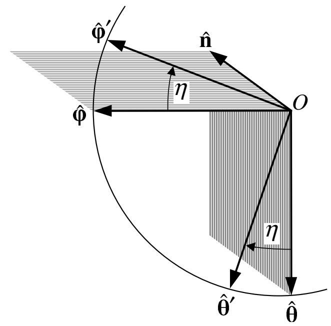


Figure 9.1: Rotation of the $\theta$- and $\varphi$-axes through an angle $\eta \ge 0$ around $\hat{\mathbf{n}}$ in the clockwise direction when looking in the direction of propagation.

## 9. Rotation transformation rule for Stokes parameters

The Stokes parameters of a plane electromagnetic wave are always defined with respect to a reference plane containing the direction of wave propagation. If the reference plane is rotated about the direction of propagation, then the Stokes parameters are modified according to a rotation transformation rule, which can be derived as follows. Consider a rotation of the coordinate axes $\theta$ and $\varphi$ through an angle $0 \le \eta < 2\pi$ in the *clockwise* direction when looking in the direction of propagation (Fig. 9.1). The transformation rule for rotation of a two-dimensional coordinate system yields

$$E'_{0\theta} = E_{0\theta}\cos\eta + E_{0\varphi}\sin\eta, \tag{9.1}$$

$$E'_{0\varphi} = -E_{0\theta}\sin\eta + E_{0\varphi}\cos\eta, \tag{9.2}$$

where the primes denote the electric field vector components with respect to the new reference frame. It then follows from Eq. (7.4) that the rotation transformation rule for the Stokes column vector is

$$\mathbf{I}' = \mathbf{L}(\eta)\mathbf{I}, \tag{9.3}$$

where

$$\mathbf{L}(\eta) = \begin{bmatrix} 1 & 0 & 0 & 0 \\ 0 & \cos 2\eta & -\sin 2\eta & 0 \\ 0 & \sin 2\eta & \cos 2\eta & 0 \\ 0 & 0 & 0 & 1 \end{bmatrix} \tag{9.4}$$

is the so-called Stokes rotation matrix for angle $\eta$. It is obvious that a $\eta = \pi$ rotation does not change the Stokes parameters.

Because

$$(\mathbf{I}^{\mathrm{MS}})' = \mathbf{B}\mathbf{I}' = \mathbf{B}\mathbf{L}(\eta)\mathbf{I} = \mathbf{B}\mathbf{L}(\eta)\mathbf{B}^{-1}\mathbf{I}^{\mathrm{MS}}, \tag{9.5}$$

the rotation matrix for the modified Stokes vector is given by

$$\mathbf{L}^{\mathrm{MS}}(\eta) = \mathbf{BL}(\eta)\mathbf{B}^{-1} = \begin{bmatrix} \cos^2\eta & \sin^2\eta & -\frac{1}{2}\sin 2\eta & 0 \\ \sin^2\eta & \cos^2\eta & \frac{1}{2}\sin 2\eta & 0 \\ \sin 2\eta & -\sin 2\eta & \cos 2\eta & 0 \\ 0 & 0 & 0 & 1 \end{bmatrix}. \tag{9.6}$$

Similarly, for the circular polarization representation,

$$(\mathbf{I}^{\mathrm{CP}})' = \mathbf{AI}' = \mathbf{AL}(\eta)\mathbf{I} = \mathbf{AL}(\eta)\mathbf{A}^{-1}\mathbf{I}^{\mathrm{CP}}, \tag{9.7}$$

and the corresponding rotation matrix is diagonal [12]:

$$\mathbf{L}^{\mathrm{CP}}(\eta) = \mathbf{AL}(\eta)\mathbf{A}^{-1} = \begin{bmatrix} \exp(\mathrm{i}2\eta) & 0 & 0 & 0 \\ 0 & 1 & 0 & 0 \\ 0 & 0 & 1 & 0 \\ 0 & 0 & 0 & \exp(-\mathrm{i}2\eta) \end{bmatrix}. \tag{9.8}$$

## 10. Quasi-monochromatic light

The definition of a monochromatic plane electromagnetic wave given by Eq. (7.1) implies that the complex amplitude $\mathbf{E}_0$ is constant. In reality, the complex amplitude often fluctuates in time, albeit much slower than the time factor $\exp(-\mathrm{i}\omega t)$. The fluctuations of the complex amplitude include, in general, fluctuations of both the amplitude and the phase of the real electric vector.

It is straightforward to verify that the electromagnetic field given by

$$\mathbf{E}(\mathbf{r},t) = \mathbf{E}_0(t)\exp(\mathrm{i}\mathbf{k}\cdot\mathbf{r} - \mathrm{i}\omega t), \tag{10.1}$$

$$\mathbf{H}(\mathbf{r},t) = \mathbf{H}_0(t)\exp(\mathrm{i}\mathbf{k}\cdot\mathbf{r} - \mathrm{i}\omega t) \tag{10.2}$$

still satisfies the Maxwell equations (2.1)–(2.4) at any moment in time provided that the medium is homogeneous and that

$$\mathbf{k}\cdot\mathbf{E}_0(t) = 0, \tag{10.3}$$

$$\mathbf{k}\cdot\mathbf{H}_0(t) = 0, \tag{10.4}$$

$$\mathbf{k}\times\mathbf{E}_0(t) = \omega\mu\mathbf{H}_0(t), \tag{10.5}$$

$$\mathbf{k}\times\mathbf{H}_0(t) = -\omega\varepsilon\mathbf{E}_0(t), \tag{10.6}$$

$$\left|\frac{\partial\mathbf{E}_0(t)}{\partial t}\right| \ll \omega|\mathbf{E}_0(t)|, \tag{10.7}$$

$$\left|\frac{\partial\mathbf{H}_0(t)}{\partial t}\right| \ll \omega|\mathbf{H}_0(t)|. \tag{10.8}$$

Equations (10.1)–(10.8) collectively define a *quasi-monochromatic* beam of light. Although the typical frequency of the fluctuations of the complex electric and magnetic field amplitudes is much smaller than the angular frequency $\omega$, it is still so high that most optical instruments are incapable of tracing the instantaneous values of the Stokes parameters but rather respond to an average of the Stokes parameters over a relatively long period of time. Therefore, the definition of the Stokes parameters for a quasi-monochromatic beam of light propagating in a homogeneous nonabsorbing medium must be modified as follows:

$$I = \frac{1}{2}\sqrt{\frac{\epsilon}{\mu}}[\langle E_{0\theta}(t)E^*_{0\theta}(t)\rangle_t + \langle E_{0\varphi}(t)E^*_{0\varphi}(t)\rangle_t], \tag{10.9}$$

$$Q = \frac{1}{2}\sqrt{\frac{\epsilon}{\mu}}[\langle E_{0\theta}(t)E^*_{0\theta}(t)\rangle_t - \langle E_{0\varphi}(t)E^*_{0\varphi}(t)\rangle_t], \tag{10.10}$$

$$U = -\frac{1}{2}\sqrt{\frac{\epsilon}{\mu}}[\langle E_{0\theta}(t)E^*_{0\varphi}(t)\rangle_t + \langle E_{0\varphi}(t)E^*_{0\theta}(t)\rangle_t], \tag{10.11}$$

$$V = \mathrm{i}\frac{1}{2}\sqrt{\frac{\epsilon}{\mu}}[\langle E_{0\varphi}(t)E^*_{0\theta}(t)\rangle_t - \langle E_{0\theta}(t)E^*_{0\varphi}(t)\rangle_t], \tag{10.12}$$

where

$$\langle f(t)\rangle_t = \frac{1}{T}\int_t^{t+T} \mathrm{d}\tau\, f(\tau) \tag{10.13}$$

denotes the average over a time interval $T$ long compared with the typical period of fluctuation.

The Stokes identity (7.8) is not, in general, valid for a quasi-monochromatic beam. Indeed, now we have

$$\begin{aligned}
&I^2 - Q^2 - U^2 - V^2 \\
&= \frac{\epsilon}{\mu}[\langle a_\theta^2\rangle_t\langle a_\varphi^2\rangle_t - \langle a_\theta a_\varphi \cos\Delta\rangle_t^2 - \langle a_\theta a_\varphi \sin\Delta\rangle_t^2] \\
&= \frac{\epsilon}{\mu}\frac{1}{T^2}\int_t^{t+T}\mathrm{d}t'\int_t^{t+T}\mathrm{d}t''\,\{[a_\theta(t')]^2[a_\varphi(t'')]^2 \\
&\qquad - a_\theta(t')a_\varphi(t')\cos[\Delta(t')]a_\theta(t'')a_\varphi(t'')\cos[\Delta(t'')] \\
&\qquad - a_\theta(t')a_\varphi(t')\sin[\Delta(t')]a_\theta(t'')a_\varphi(t'')\sin[\Delta(t'')]\} \\
&= \frac{\epsilon}{\mu}\frac{1}{T^2}\int_t^{t+T}\mathrm{d}t'\int_t^{t+T}\mathrm{d}t''\,\{[a_\theta(t')]^2[a_\varphi(t'')]^2 \\
&\qquad - a_\theta(t')a_\varphi(t')a_\theta(t'')a_\varphi(t'')\cos[\Delta(t') - \Delta(t'')]\} \\
&= \frac{\epsilon}{\mu}\frac{1}{2T^2}\int_t^{t+T}\mathrm{d}t'\int_t^{t+T}\mathrm{d}t''\,\{[a_\theta(t')]^2[a_\varphi(t'')]^2 + [a_\theta(t'')]^2[a_\varphi(t')]^2 \\
&\qquad - 2a_\theta(t')a_\varphi(t')a_\theta(t'')a_\varphi(t'')\cos[\Delta(t') - \Delta(t'')]\}
\end{aligned}$$

$$\geq \frac{\epsilon}{\mu}\frac{1}{2T^2}\int_t^{t+T}\mathrm{d}t'\int_t^{t+T}\mathrm{d}t''\,\{[a_\theta(t')]^2[a_\varphi(t'')]^2 + [a_\theta(t'')]^2[a_\varphi(t')]^2 - 2a_\vartheta(t')a_\varphi(t')a_\vartheta(t'')a_\varphi(t'')\}$$
$$= \frac{\epsilon}{\mu}\frac{1}{2T^2}\int_t^{t+T}\mathrm{d}t'\int_t^{t+T}\mathrm{d}t''\,[a_\theta(t')a_\varphi(t'') - a_\theta(t'')a_\varphi(t')]^2$$
$$\geq 0, \tag{10.14}$$

thereby yielding

$$I^2 \geq Q^2 + U^2 + V^2. \tag{10.15}$$

The equality holds only if the ratio $a_\theta(t)/a_\varphi(t)$ of the real amplitudes and the phase difference $\Delta(t)$ are independent of time, which means that $E_{0\theta}(t)$ and $E_{0\varphi}(t)$ are completely correlated. In this case the beam is said to be fully (or completely) polarized. This definition includes a monochromatic plane wave, but is, of course, more general. On the other hand, if $a_\theta(t)$, $a_\varphi(t)$, $\Delta_\theta(t)$, and $\Delta_\varphi(t)$ are totally uncorrelated and $\langle a_\theta^2\rangle_t = \langle a_\varphi^2\rangle_t$ then $Q = U = V = 0$, and the quasi-monochromatic beam of light is said to be unpolarized (or natural). This means that the parameters of the vibration ellipse traced by the endpoint of the electric vector fluctuate in such a way that there is no preferred vibration ellipse.

When two or more quasi-monochromatic beams propagating in the same direction are mixed incoherently, which means that there is no permanent phase relation between the separate beams, then the Stokes vector of the mixture is equal to the sum of the Stokes vectors of the individual beams:

$$\mathbf{I} = \sum_n \mathbf{I}_n, \tag{10.16}$$

where $n$ numbers the beams. Indeed, inserting Eqs. (8.1) and (8.2) in Eq. (10.9), we obtain for the total intensity

$$I = \frac{1}{2}\sqrt{\frac{\epsilon}{\mu}}\sum_n\sum_m \langle a_{\theta n}a_{\theta m}\exp[\mathrm{i}(\Delta_{\theta n} - \Delta_{\theta m})] + a_{\varphi n}a_{\varphi m}\exp[\mathrm{i}(\Delta_{\varphi n} - \Delta_{\varphi m})]\rangle_t$$
$$= \frac{1}{2}\sqrt{\frac{\epsilon}{\mu}}\Big\{\sum_n I_n + \sum_n\sum_{m\neq n}\langle a_{\theta n}a_{\theta m}\exp[\mathrm{i}(\Delta_{\theta n} - \Delta_{\theta m})] + a_{\varphi n}a_{\varphi m}\exp[\mathrm{i}(\Delta_{\varphi n} - \Delta_{\varphi m})]\rangle_t\Big\}. \tag{10.17}$$

Since the phases of different beams are uncorrelated, the second term on the right-hand side of the relation above vanishes. Hence

$$I = \sum_n I_n, \tag{10.18}$$

and similarly for $Q$, $U$, and $V$. Of course, this additivity rule also applies to the coherency matrix $\boldsymbol{\rho}$, the modified Stokes vector $\mathbf{I}^{\mathrm{MS}}$, and the circular-polarization vector $\mathbf{I}^{\mathrm{CP}}$.

The additivity of the Stokes parameters allows us to generalize the principle of optical equivalence (Section 7) to quasi-monochromatic light as follows: it is impossible by means of a traditional optical instrument to distinguish between various incoherent mixtures of quasi-monochromatic beams that form a beam with the same Stokes parameters $(I, Q, U, V)$. For example, there is only one kind of unpolarized light, although it can be composed of quasi-monochromatic beams in an infinite variety of optically indistinguishable ways.

According to Eqs. (10.15) and (10.16), it always is possible *mathematically* to decompose any quasi-monochromatic beam into two incoherent parts, one unpolarized with a Stokes vector

$$[I - \sqrt{Q^2 + U^2 + V^2} \quad 0 \quad 0 \quad 0]^{\mathrm{T}},$$

and one fully polarized, with a Stokes vector

$$[\sqrt{Q^2 + U^2 + V^2} \quad Q \quad U \quad V]^{\mathrm{T}}.$$

Thus, the intensity of the fully polarized component is $\sqrt{Q^2 + U^2 + V^2}$, so that the degree of (elliptical) polarization of the quasi-monochromatic beam is

$$P = \frac{\sqrt{Q^2 + U^2 + V^2}}{I}. \tag{10.19}$$

The degree of linear polarization is defined as

$$P_{\mathrm{L}} = \sqrt{Q^2 + U^2} \Big/ I \tag{10.20}$$

and the degree of circular polarization as

$$P_{\mathrm{C}} = \frac{V}{I}. \tag{10.21}$$

$P$ vanishes for unpolarized light and is equal to unity for fully polarized light. For a partially polarized beam ($0 < P < 1$) with $V \neq 0$, the sign of $V$ indicates the preferential handedness of the vibration ellipses described by the endpoint of the electric vector. Specifically, a positive $V$ indicates left-handed polarization and a negative $V$ indicates right-handed polarization. By analogy with Eqs. (8.28) and (8.29), the quantities $-U/Q$ and $|V| \Big/ \sqrt{Q^2 + U^2}$ can be interpreted as specifying the preferential orientation and ellipticity of the

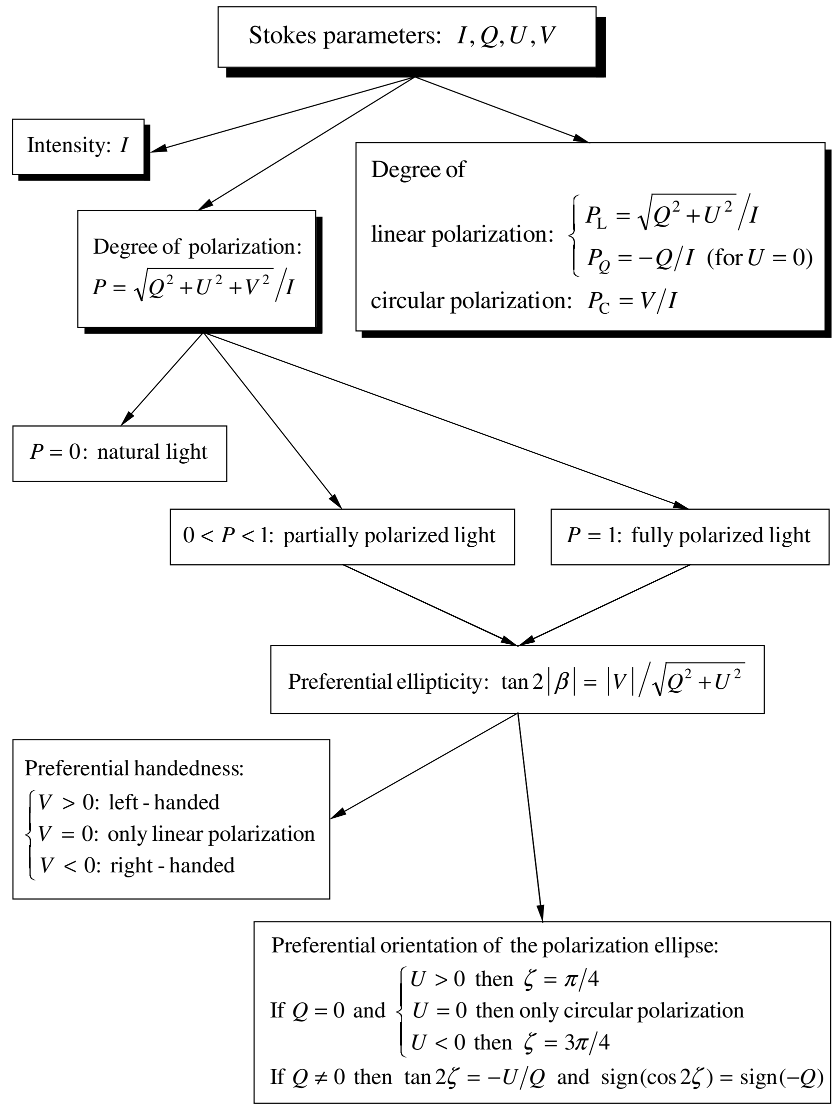


Figure 10.1: Analysis of a quasi-monochromatic beam with Stokes parameters *I*, *Q*, *U*, and *V*.

vibration ellipse. Unlike the Stokes parameters, these quantities are not additive. According to Eqs. (9.3) and (9.4), the $P$, $P_L$, and $P_C$ are invariant with respect to rotations of the reference frame around the direction of propagation.

When $U = 0$, the ratio

$$P_Q = -\frac{Q}{I} \tag{10.22}$$

is also called the degree of linear polarization (or the *signed* degree of linear polarization). $P_Q$ is positive when the vibrations of the electric vector in the $\varphi$-direction (i.e., in the direction perpendicular to the meridional plane of the beam) dominate those in the $\theta$-direction, and is negative otherwise.

The standard polarimetric analysis of a general quasi-monochromatic beam with Stokes parameters *I*, *Q*, *U*, and *V* is summarized in Fig. 10.1.

## 11. Measurement of the Stokes parameters

Most detectors of electromagnetic radiation, especially those in the visible and infrared spectral range, are insensitive to the polarization state of the beam impinging on the detector surface and can measure only the first Stokes parameter of the beam, viz., the intensity. Therefore, to measure the entire Stokes vector of the beam, one has to insert between the source of light and the detector one or several optical elements that modify the first Stokes parameter of the radiation reaching the detector in such a way that it contains information about the second, third, and fourth Stokes parameters of the original beam. This is usually done with so called polarizers and retarders.

A polarizer is an optical element that attenuates the orthogonal components of the electric field vector of an electromagnetic wave unevenly. Let us denote the corresponding attenuation coefficients as $p_\theta$ and $p_\varphi$ and consider first the situation when the two orthogonal transmission axes of a polarizer coincide with the $\theta$- and $\varphi$-axes of the laboratory coordinate system (see Fig. 11.1). This means that after the electromagnetic wave goes through the polarizer, the orthogonal components of the electric field change as follows:

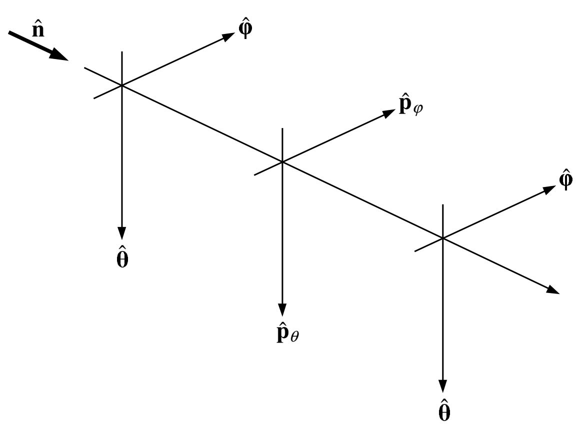


Figure 11.1: The transmission axes of the polarizer coincide with those of the laboratory reference frame.

$$E'_\theta = p_\theta E_\theta, \quad 0 \le p_\theta \le 1, \tag{11.1}$$

$$E'_\varphi = p_\varphi E_\varphi, \quad 0 \le p_\varphi \le 1. \tag{11.2}$$

It then follows from the definition of the Stokes parameters that the Stokes vector of the wave modifies according to

$$\mathbf{I}' = \mathbf{P}\mathbf{I}, \tag{11.3}$$

where

$$\mathbf{P} = \frac{1}{2}\begin{bmatrix} p_\theta^2 + p_\varphi^2 & p_\theta^2 - p_\varphi^2 & 0 & 0 \\ p_\theta^2 - p_\varphi^2 & p_\theta^2 + p_\varphi^2 & 0 & 0 \\ 0 & 0 & 2p_\theta p_\varphi & 0 \\ 0 & 0 & 0 & 2p_\theta p_\varphi \end{bmatrix} \tag{11.4}$$

is the so-called Mueller matrix of the polarizer.

An important example of a polarizer is a neutral filter with $p_\theta = p_\varphi = p$, which equally attenuates the orthogonal components of the electric field vector and does not change the polarization state of the wave:

$$\mathbf{P} = p^2\begin{bmatrix} 1 & 0 & 0 & 0 \\ 0 & 1 & 0 & 0 \\ 0 & 0 & 1 & 0 \\ 0 & 0 & 0 & 1 \end{bmatrix}. \tag{11.5}$$

In contrast, an ideal linear polarizer transmits only one orthogonal component of the wave (say, the $\theta$ component) and completely blocks the other one $(p_\varphi = 0)$:

$$\mathbf{P} = \frac{p_\theta^2}{2}\begin{bmatrix} 1 & 1 & 0 & 0 \\ 1 & 1 & 0 & 0 \\ 0 & 0 & 0 & 0 \\ 0 & 0 & 0 & 0 \end{bmatrix}. \tag{11.6}$$

An ideal perfect linear polarizer does not change one orthogonal component $(p_\theta = 1)$ and completely blocks the other one $(p_\varphi = 0)$:

$$\mathbf{P} = \frac{1}{2}\begin{bmatrix} 1 & 1 & 0 & 0 \\ 1 & 1 & 0 & 0 \\ 0 & 0 & 0 & 0 \\ 0 & 0 & 0 & 0 \end{bmatrix}. \tag{11.7}$$

If the transmission axes of a polarizer are rotated relative to the laboratory coordinate system (Fig. 11.2) then its Mueller matrix with respect to the laboratory coordinate system also changes. To obtain the resulting Stokes vector with respect to the laboratory coordinate system, we need to

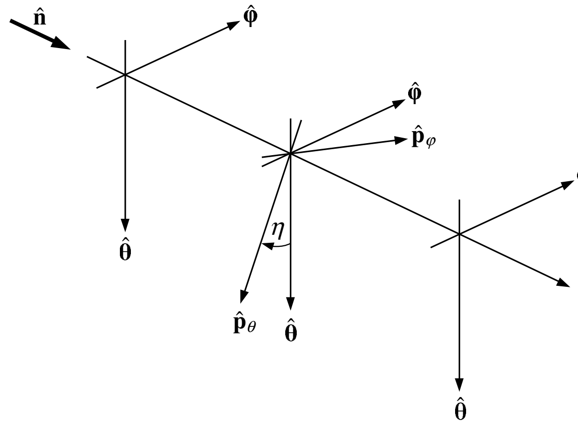


Figure 11.2: The polarizer transmission axes are rotated through an angle $\eta \geq 0$ around $\hat{\mathbf{n}}$ in the clockwise direction when looking in the direction of propagation.

1. "rotate" the initial Stokes vector through the angle $\eta$ in the clockwise direction in order to obtain the Stokes parameters of the original beam with respect to the polarizer axes;
2. multiply the "rotated" Stokes vector by the original (non-rotated) polarizer Mueller matrix; and finally
3. "rotate" the Stokes vector thus obtained through the angle $-\eta$ in order to calculate the Stokes parameters of the resulting beam with respect to the laboratory coordinate system.

The final result is as follows:

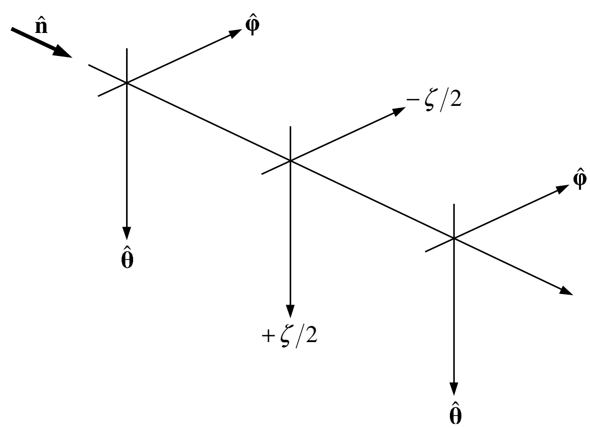


Figure 11.3: Propagation of a beam through a retarder.

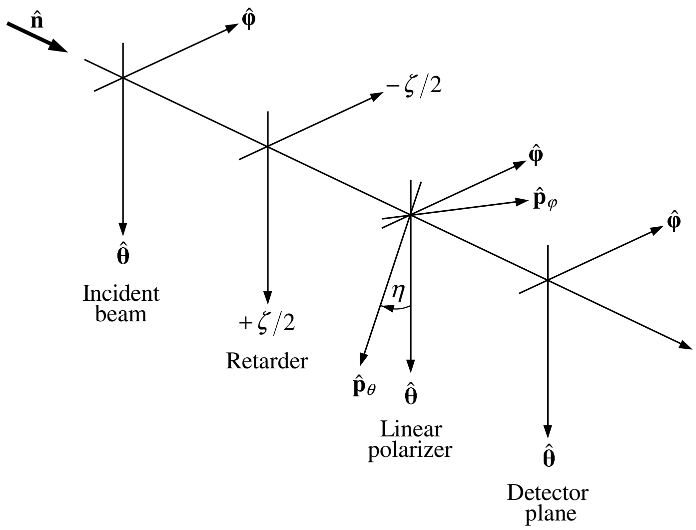


Figure 11.4: Measurement of the Stokes parameters with a retarder and an ideal perfect linear polarizer rotated with respect to the laboratory reference frame.

$$\mathbf{I}' = \mathbf{L}(-\eta)\mathbf{P}\mathbf{L}(\eta)\mathbf{I}. \tag{11.8}$$

Hence the Mueller matrix of the rotated polarizer computed with respect to the laboratory coordinate system is given by

$$\mathbf{P}(\eta) = \mathbf{L}(-\eta)\mathbf{P}\mathbf{L}(\eta) \tag{11.9}$$

with $\mathbf{P}(0) = \mathbf{P}$.

A retarder is an optical element that changes the phase of the beam by causing a phase shift of $+\zeta/2$ along the $\theta$-axis and a phase shift of $-\zeta/2$ along the $\varphi$-axis (Fig. 11.3). We thus have

$$E'_\theta = \exp(+\mathrm{i}\zeta/2)E_\theta, \tag{11.10}$$

$$E'_\varphi = \exp(-\mathrm{i}\zeta/2)E_\varphi, \tag{11.11}$$

which yields

$$\mathbf{I}' = \mathbf{R}(\zeta)\mathbf{I}, \tag{11.12}$$

where

$$\mathbf{R}(\zeta) = \begin{bmatrix} 1 & 0 & 0 & 0 \\ 0 & 1 & 0 & 0 \\ 0 & 0 & \cos\zeta & \sin\zeta \\ 0 & 0 & -\sin\zeta & \cos\zeta \end{bmatrix} \tag{11.13}$$

is the Mueller matrix of the retarder.

Consider now the optical path shown in Fig. 11.4. The beam of light goes through a retarder and a rotated ideal perfect linear polarizer and then impinges on the surface of a polarization-insensitive detector. The Stokes vector of the resulting beam impinging on the detector surface is given by

$$\mathbf{I}' = \mathbf{P}(\eta)\mathbf{R}(\zeta)\mathbf{I}, \tag{11.14}$$

where the polarizer Mueller matrix is

$$\mathbf{P}(\eta) = \frac{1}{2}\begin{bmatrix} 1 & \cos 2\eta & -\sin 2\eta & 0 \\ \cos 2\eta & \cos^2 2\eta & -\cos 2\eta \sin 2\eta & 0 \\ -\sin 2\eta & -\cos 2\eta \sin 2\eta & \sin^2 2\eta & 0 \\ 0 & 0 & 0 & 0 \end{bmatrix} \tag{11.15}$$

(cf. Eqs. (11.7) and (11.9)). Hence the intensity of the resulting beam as a function of $\eta$ and $\zeta$ is given by

$$I'(\eta, \zeta) = \tfrac{1}{2}(I + Q\cos 2\eta - U \sin 2\eta \cos\zeta - V \sin 2\eta \sin\zeta). \tag{11.16}$$

This formula suggests a simple way to determine the Stokes parameters of the original beam by measuring the intensity of the resulting beam using four different combinations of $\eta$ and $\zeta$ :

$$I = I'(0°, 0°) + I'(90°, 0°), \tag{11.17}$$

$$Q = I'(0°, 0°) - I'(90°, 0°), \tag{11.18}$$

$$U = -2I'(45°, 0°) + I, \tag{11.19}$$

$$V = I - 2I'(45°, 90°). \tag{11.20}$$

Other methods for measuring the Stokes parameters and practical aspects of polarimetry are discussed in detail in [14–17].

## 12. Spherical wave solution

As we have seen, plane electromagnetic waves represent a fundamental solution of the Maxwell equations underlying the concept of a monochromatic parallel beam of light. Another fundamental solution representing the outward propagation of electromagnetic energy from a point-like source is a transverse spherical wave. To derive this solution, we need Eqs. (4.3), (4.4), (4.11), (4.16), (4.17), (6.1), and (6.2) as well as the following formulas:

$$\nabla \frac{\exp(\mathrm{i}kr)}{r} = \left(\mathrm{i}k - \frac{1}{r}\right)\frac{\exp(\mathrm{i}kr)}{r}\hat{\mathbf{r}}, \tag{12.1}$$

$$\nabla \cdot \mathbf{a} = \frac{\partial a_r}{\partial r} + \frac{2a_r}{r} + \frac{1}{r}\frac{\partial a_\theta}{\partial \theta} + \frac{a_\theta}{r\tan\theta} + \frac{1}{r\sin\theta}\frac{\partial a_\varphi}{\partial \varphi}, \tag{12.2}$$

$$
\begin{aligned}
\nabla\times\mathbf{a} &= \left(\frac{1}{r}\frac{\partial a_\varphi}{\partial\theta} + \frac{a_\varphi}{r\tan\theta} - \frac{1}{r\sin\theta}\frac{\partial a_\theta}{\partial\varphi}\right)\hat{\mathbf{r}} \\
&+ \left(\frac{1}{r\sin\theta}\frac{\partial a_r}{\partial\varphi} - \frac{\partial a_\varphi}{\partial r} - \frac{a_\varphi}{r}\right)\hat{\boldsymbol{\theta}} \\
&+ \left(\frac{\partial a_\theta}{\partial r} + \frac{a_\theta}{r} - \frac{1}{r}\frac{\partial a_r}{\partial\theta}\right)\hat{\boldsymbol{\varphi}}. \qquad (12.3)
\end{aligned}
$$

It is then straightforward to verify that the complex field vectors

$$\mathbf{E}(\mathbf{r},t) = \frac{\exp(\mathrm{i}kr)}{r}\mathbf{E}_1(\hat{\mathbf{r}})\exp(-\mathrm{i}\omega t), \qquad (12.4)$$

$$\mathbf{H}(\mathbf{r},t) = \frac{\exp(\mathrm{i}kr)}{r}\mathbf{H}_1(\hat{\mathbf{r}})\exp(-\mathrm{i}\omega t) \qquad (12.5)$$

are a solution of the Maxwell equations in the limit $kr \to \infty$ provided that the medium is homogeneous and that

$$\hat{\mathbf{r}}\cdot\mathbf{E}_1(\hat{\mathbf{r}}) = 0, \qquad (12.6)$$

$$\hat{\mathbf{r}}\cdot\mathbf{H}_1(\hat{\mathbf{r}}) = 0, \qquad (12.7)$$

$$k\hat{\mathbf{r}}\times\mathbf{E}_1(\hat{\mathbf{r}}) = \omega\mu\mathbf{H}_1(\hat{\mathbf{r}}), \qquad (12.8)$$

$$k\hat{\mathbf{r}}\times\mathbf{H}_1(\hat{\mathbf{r}}) = -\omega\varepsilon\mathbf{E}_1(\hat{\mathbf{r}}), \qquad (12.9)$$

where the wavenumber $k = k_\mathrm{R} + \mathrm{i}k_\mathrm{I} = \omega\sqrt{\varepsilon\mu} = \omega m/c$ may be complex and the $\mathbf{E}_1(\hat{\mathbf{r}})$ and $\mathbf{H}_1(\hat{\mathbf{r}})$ are independent of the distance $r$ from the origin.

Equations (12.4)–(12.9) describe an outgoing transverse spherical wave propagating radially with the phase velocity $v = \omega/k_\mathrm{R}$ and having mutually perpendicular complex electric and magnetic field vectors. The wave is homogeneous in that the real and imaginary parts of the complex wave vector $k\hat{\mathbf{r}}$ are parallel. The surfaces of constant phase coincide with the surfaces of constant amplitude and are spherical. Obviously,

$$\mathbf{H}(\mathbf{r},t) = \frac{k}{\omega\mu}\hat{\mathbf{r}}\times\mathbf{E}(\mathbf{r},t), \qquad (12.10)$$

which allows one to consider the spherical wave in terms of the electric (or magnetic) field only. The time-averaged Poynting vector of the wave is given by

$$\langle \mathcal{S}(\mathbf{r},t)\rangle_t = \tfrac{1}{2}\mathrm{Re}\left(\sqrt{\frac{\varepsilon}{\mu}}\right)\frac{|\mathbf{E}_1(\hat{\mathbf{r}})|^2}{r^2}\exp\left(-2\frac{\omega}{c}m_\mathrm{I}r\right)\hat{\mathbf{r}}, \qquad (12.11)$$

where, as before, $m_\mathrm{I} = ck_\mathrm{I}/\omega$. The intensity of the spherical wave is defined

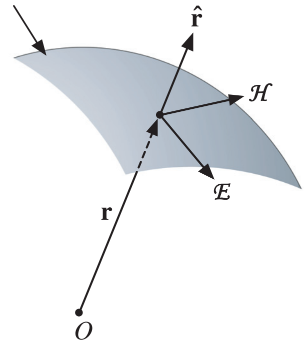


Figure 12.1: Spherical electromagnetic wave propagating in a homogeneous medium with no dispersion and losses.

as the absolute value of the time-averaged Poynting vector,

$$I(\mathbf{r}) = \left|\langle \mathcal{S}(\mathbf{r},t)\rangle_t\right| = \tfrac{1}{2}\mathrm{Re}\left(\sqrt{\frac{\varepsilon}{\mu}}\right)\frac{\left|\mathbf{E}_1(\hat{\mathbf{r}})\right|^2}{r^2}\exp\left(-2\frac{\omega}{c}m_{\mathrm{I}}r\right). \quad (12.12)$$

The intensity has the dimension of monochromatic energy flux and specifies the amount of electromagnetic energy crossing a unit surface element normal to $\hat{\mathbf{r}}$ per unit time. The intensity is attenuated exponentially by absorption and in addition decreases as the inverse square of the distance from the origin.

In the case of a medium with no dispersion and losses, the real electric and magnetic field vectors are mutually orthogonal and are normal to the direction of propagation $\hat{\mathbf{r}}$ (Fig. 12.1). The energy conservation law takes the form

$$\begin{aligned}\oint_S \mathrm{d}S\langle \mathcal{S}(\mathbf{r},t)\rangle_t\cdot\hat{\mathbf{r}} &= \oint_S \mathrm{d}S I(\mathbf{r})\\ &= \frac{1}{2}\sqrt{\frac{\epsilon}{\mu}}\frac{1}{r^2}\oint_S \mathrm{d}S\left|\mathbf{E}_1(\hat{\mathbf{r}})\right|^2\\ &= \frac{1}{2}\sqrt{\frac{\epsilon}{\mu}}\int_{4\pi}\mathrm{d}\hat{\mathbf{r}}\left|\mathbf{E}_1(\hat{\mathbf{r}})\right|^2\\ &= \text{constant}, \end{aligned} \quad (12.13)$$

where $S$ is the sphere of radius $r$ and

$$\mathrm{d}\hat{\mathbf{r}} = \frac{\mathrm{d}S}{r^2} = \sin\theta\,\mathrm{d}\theta\,\mathrm{d}\varphi \quad (12.14)$$

is an infinitesimal solid angle element around the direction $\hat{\mathbf{r}}$. It is also easy to show that in the case of a nonabsorbing medium, the time-averaged energy density of a spherical wave is given by

$$\langle u(\mathbf{r},t)\rangle_t = \tfrac{1}{2}\epsilon \frac{|\mathbf{E}_1(\hat{\mathbf{r}})|^2}{r^2}. \tag{12.15}$$

Equations (12.12) and (12.15) show that $I(\mathbf{r}) = v\langle u(\mathbf{r},t)\rangle_t$, where $v = 1/\sqrt{\epsilon\mu}$ is the speed of light in the material medium. This is the same result as that obtained previously for a plane wave propagating in a nonabsorbing medium (cf. Eq. (6.30)).

In complete analogy with the case of a plane wave, the coherency matrix, the coherency column vector, and the Stokes column vector of a spherical wave propagating in a homogeneous medium with no dispersion and losses can be defined as

$$\boldsymbol{\rho}(\mathbf{r}) = \begin{bmatrix} \rho_{11}(\mathbf{r}) & \rho_{12}(\mathbf{r}) \\ \rho_{21}(\mathbf{r}) & \rho_{22}(\mathbf{r}) \end{bmatrix} = \frac{1}{2}\sqrt{\frac{\epsilon}{\mu}}\frac{1}{r^2}\begin{bmatrix} E_{1\theta}(\hat{\mathbf{r}})E^*_{1\theta}(\hat{\mathbf{r}}) & E_{1\theta}(\hat{\mathbf{r}})E^*_{1\varphi}(\hat{\mathbf{r}}) \\ E_{1\varphi}(\hat{\mathbf{r}})E^*_{1\theta}(\hat{\mathbf{r}}) & E_{1\varphi}(\hat{\mathbf{r}})E^*_{1\varphi}(\hat{\mathbf{r}}) \end{bmatrix}, \tag{12.16}$$

$$\mathbf{J}(\mathbf{r}) = \begin{bmatrix} \rho_{11}(\mathbf{r}) \\ \rho_{12}(\mathbf{r}) \\ \rho_{21}(\mathbf{r}) \\ \rho_{22}(\mathbf{r}) \end{bmatrix} = \frac{1}{2}\sqrt{\frac{\epsilon}{\mu}}\frac{1}{r^2}\begin{bmatrix} E_{1\theta}(\hat{\mathbf{r}})E^*_{1\theta}(\hat{\mathbf{r}}) \\ E_{1\theta}(\hat{\mathbf{r}})E^*_{1\varphi}(\hat{\mathbf{r}}) \\ E_{1\varphi}(\hat{\mathbf{r}})E^*_{1\theta}(\hat{\mathbf{r}}) \\ E_{1\varphi}(\hat{\mathbf{r}})E^*_{1\varphi}(\hat{\mathbf{r}}) \end{bmatrix}, \tag{12.17}$$

$$\mathbf{I}(\mathbf{r}) = \begin{bmatrix} I(\mathbf{r}) \\ Q(\mathbf{r}) \\ U(\mathbf{r}) \\ V(\mathbf{r}) \end{bmatrix} = \mathbf{DJ}(\mathbf{r}) = \frac{1}{2}\sqrt{\frac{\epsilon}{\mu}}\frac{1}{r^2}\begin{bmatrix} E_{1\theta}(\hat{\mathbf{r}})E^*_{1\theta}(\hat{\mathbf{r}}) + E_{1\varphi}(\hat{\mathbf{r}})E^*_{1\varphi}(\hat{\mathbf{r}}) \\ E_{1\theta}(\hat{\mathbf{r}})E^*_{1\theta}(\hat{\mathbf{r}}) - E_{1\varphi}(\hat{\mathbf{r}})E^*_{1\varphi}(\hat{\mathbf{r}}) \\ -E_{1\theta}(\hat{\mathbf{r}})E^*_{1\varphi}(\hat{\mathbf{r}}) - E_{1\varphi}(\hat{\mathbf{r}})E^*_{1\theta}(\hat{\mathbf{r}}) \\ \mathrm{i}[E_{1\varphi}(\hat{\mathbf{r}})E^*_{1\theta}(\hat{\mathbf{r}}) - E_{1\theta}(\hat{\mathbf{r}})E^*_{1\varphi}(\hat{\mathbf{r}})] \end{bmatrix}, \tag{12.18}$$

respectively. All these quantities have the dimension of monochromatic energy flux. As before, the first Stokes parameter is the intensity (defined this time by Eq. (12.12)).

## 13. Coherency dyad

The definition of the coherency and Stokes vectors explicitly exploits the transverse character of an electromagnetic wave and requires the use of a local spherical coordinate system. However, in some cases it is convenient to introduce an alternative quantity, which also provides a complete optical specification of a transverse electromagnetic wave, but is defined without explicit use of a coordinate system. This quantity is called the coherency dyad and, in the general case of an arbitrary electromagnetic field, is given by

$$\vec{\rho}(\mathbf{r},t) = \mathbf{E}(\mathbf{r},t) \otimes \mathbf{E}^*(\mathbf{r},t), \tag{13.1}$$

where $\otimes$ denotes the dyadic product of two vectors. It is then clear that the coherency and Stokes vectors of a transverse time-harmonic electromagnetic wave can be expressed in terms of the coherency dyad as follows:

$$\mathsf{J} = \frac{1}{2}\sqrt{\frac{\varepsilon}{\mu}} \begin{bmatrix} \hat{\boldsymbol{\theta}} \cdot \vec{\rho} \cdot \hat{\boldsymbol{\theta}} \\ \hat{\boldsymbol{\theta}} \cdot \vec{\rho} \cdot \hat{\boldsymbol{\varphi}} \\ \hat{\boldsymbol{\varphi}} \cdot \vec{\rho} \cdot \hat{\boldsymbol{\theta}} \\ \hat{\boldsymbol{\varphi}} \cdot \vec{\rho} \cdot \hat{\boldsymbol{\varphi}}) \end{bmatrix}, \tag{13.2}$$

$$\mathsf{I} = \frac{1}{2}\sqrt{\frac{\varepsilon}{\mu}} \begin{bmatrix} \hat{\boldsymbol{\theta}} \cdot \vec{\rho} \cdot \hat{\boldsymbol{\theta}} + \hat{\boldsymbol{\varphi}} \cdot \vec{\rho} \cdot \hat{\boldsymbol{\varphi}} \\ \hat{\boldsymbol{\theta}} \cdot \vec{\rho} \cdot \hat{\boldsymbol{\theta}} - \hat{\boldsymbol{\varphi}} \cdot \vec{\rho} \cdot \hat{\boldsymbol{\varphi}} \\ -\hat{\boldsymbol{\theta}} \cdot \vec{\rho} \cdot \hat{\boldsymbol{\varphi}} - \hat{\boldsymbol{\varphi}} \cdot \vec{\rho} \cdot \hat{\boldsymbol{\theta}} \\ \mathrm{i}(\hat{\boldsymbol{\varphi}} \cdot \vec{\rho} \cdot \hat{\boldsymbol{\theta}} - \hat{\boldsymbol{\theta}} \cdot \vec{\rho} \cdot \hat{\boldsymbol{\varphi}}) \end{bmatrix}, \tag{13.3}$$

whereas the products $\vec{\rho} \cdot \hat{\mathbf{n}}$ and $\hat{\mathbf{n}} \cdot \vec{\rho}$ vanish. It follows from the definition of the coherency dyad that it is Hermitian:

$$(\vec{\rho})^{\mathrm{T}} = \rho^*. \tag{13.4}$$

The coherency dyad is a more general quantity than the coherency and Stokes vectors because it can be applied to any electromagnetic field and not just to a transverse electromagnetic wave. The simplest example of a situation in which the coherency dyad can be introduced, whereas the Stokes vector cannot involves the superposition of two plane electromagnetic waves propagating in different directions. The more general nature of the coherency dyad makes the latter very convenient in studies of random electromagnetic fields created by large stochastic groups of scatterers. For example, the additivity of the Stokes parameters (Section 10) is a concept that can be applied only to transverse waves propagating in exactly the same direction, whereas the average coherency dyad of a random electromagnetic field at an observation point can sometimes be reduced to an incoherent sum of coherency dyads of transverse waves propagating in various directions [18,19].

It is important to remember, however, that when the coherency dyad is applied to an arbitrary electromagnetic field, it may not always have as definite a physical meaning as, for example, the Poynting vector. The relationship between the coherency dyad and the actual physical observables may change depending on the problem at hand and must be established carefully whenever this quantity is used in a theoretical analysis of a specific measurement procedure. For example, the right-hand sides of Eqs. (13.2) and (13.3) may become rather meaningless if the products $\vec{\rho} \cdot \hat{\mathbf{n}}$ and $\hat{\mathbf{n}} \cdot \vec{\rho}$ do not vanish.

## 14. Historical notes and further reading

The equations of classical electromagnetics were written originally by James Clerk Maxwell (1831–1979) in Cartesian component form [20] and were cast in the modern vector form by Oliver Heaviside (1850–1925). The subsequent experimental verification of Maxwell's theory by Heinrich Rudolf Hertz (1857–1894) made it a well-established discipline. Since then classical electromagnetics has been a cornerstone of physics and has played a critical role in the development of a great variety of scientific, engineering, and biomedical disciplines. The fundamental nature of Maxwell's electromagnetics was ultimately asserted by the development of the special theory of relativity by Jules Henri Poincaré (1854–1912) and Hendrik Antoon Lorentz (1853–1928).

Sir George Gabriel Stokes (1819–1903) was the first to discover that four parameters, now known as the Stokes parameters, could characterize the polarization state of any light beam, including partially polarized and unpolarized light [13]. Furthermore, he noted that unlike the quantities entering the amplitude formulation of the optical field, these parameters could be directly measured by a suitable optical instrument. The fascinating subject of polarization had attracted the attention of many other great scientists before and after Stokes, including Augustin Jean Fresnel (1788–1827), Dominique François Arago (1786–1853), Thomas Young (1773–1829), Subrahmanyan Chandrasekhar (1910–1995), and Hendrik van de Hulst (1918–2000). Even Poincaré, who is rightfully considered to be one the greatest geniuses of all time, could not help but contribute to this discipline by developing a useful polarization analysis tool now known as the Poincaré sphere [21].

The two-volume monograph by Sir Edmund Whittaker [22] remains by far the most complete and balanced account of the history of electromagnetism from the time of William Gilbert (1544–1603) and René Descartes (1596–1650) to the relativity theory. This magnificent work should be read by everyone interested in a masterful and meticulously documented recreation of the sequence of events and publications that shaped physics as we know it. In this era of endless attempts to rewrite the history of modern physics by ignorant and/or biased authors (including those of the numerous guides for "dummies"), many of whom could not be bothered to study the original sources and barely could understand the subject matter, the monumental treatise by Whittaker is an ideal starting point for those individuals who want to form their own opinions as it provides a presentation of facts rather gossip, prejudices, and intentional distortions.

Comprehensive modern accounts of classical electromagnetics and optics can be found in [1,2,7]. Extensive treatments of theoretical and experimental polarimetry were provided by Shurcliff [14], Azzam and Bashra [15], Kliger *et al.* [16], and Collett [17]. Pye [23] describes numerous manifestations of polarization in science and nature.

**Acknowledgments**

We thank Joop Hovenier and Gorden Videen for many useful discussions and Nadia Zakharova for help with graphics. This research was funded by the NASA Radiation Sciences Program managed by Donald Anderson.

**References**

1. J. D. Jackson (1998). *Classical Electrodynamics* (John Wiley & Sons, New York).
2. M. Born and E. Wolf (1999). *Principles of Optics* (Cambridge University Press, Cambridge).
3. C. F. Bohren and D. R. Huffman (1983). *Absorption and Scattering of Light by Small Particles* (John Wiley & Sons, New York).
4. P. W. Barber and S. C. Hill (1990). *Light Scattering by Particles: Computational Methods* (World Scientific, Singapore).
5. M. I. Mishchenko, J. W. Hovenier, and L. D. Travis, eds. (2000). *Light Scattering by Nonspherical Particles: Theory, Measurements, and Applications* (Academic Press, San Diego).
6. M. I. Mishchenko, L. D. Travis, and A. A. Lacis (2002). *Scattering, Absorption, and Emission of Light by Small Particles* (Cambridge University Press, Cambridge).
7. J. A. Stratton (1941). *Electromagnetic Theory* (McGraw Hill, New York).
8. L. Tsang, J. A. Kong, and K.-H. Ding (2000). *Scattering of Electromagnetic Waves: Theories and Applications* (John Wiley & Sons, New York).
9. J. A. Kong (2000). *Electromagnetic Wave Theory* (EMW Publishing, Cambridge, MA).
10. H. C. van de Hulst (1957). *Light Scattering by Small Particles* (John Wiley & Sons, New York).
11. M. Kerker (1969). *The Scattering of Light and Other Electromagnetic Radiation* (Academic Press, San Diego).
12. J. W. Hovenier and C. V. M. van der Mee (1983). Fundamental relationships relevant to the transfer of polarized light in a scattering atmosphere. *Astron. Astrophys.* **128**, 1–16.
13. G. G. Stokes (1852). On the composition and resolution of streams of polarized light from different sources. *Trans. Cambridge Philos. Soc.* **9**, 399–416.
14. W. A. Shurcliff (1962). *Polarized Light: Production and Use* (Harvard University Press, Cambridge, MA).
15. R. M. A. Azzam and N. M. Bashara (1977). *Ellipsometry and Polarized Light* (North Holland, Amsterdam).
16. D. S. Kliger, J. W. Lewis, and C. E. Randall (1990). *Polarized Light in Optics and Spectroscopy* (Academic Press, San Diego).
17. E. Collett (1992). *Polarized Light: Fundamentals and Applications* (Marcel Dekker, New York).
18. M. I. Mishchenko (2002). Vector radiative transfer equation for arbitrarily shaped and arbitrarily oriented particles: a microphysical derivation from statistical electromagnetics. *Appl. Opt.* **41**, 7114–7134.
19. M. I. Mishchenko (2003). Microphysical approach to polarized radiative transfer: extension to the case of an external observation point. *Appl. Opt.* **42**, 4963– 4967.
20. J. Clerk Maxwell (1891). *A Treatise on Electricity and Magnetism* (Clarendon Press, Oxford) (reprinted by Dover, New York, 1954).
21. H. Poincaré (1892). *Théorie Mathématique de la Lumière*, Vol. 2 (Georges Carré, Paris).

22. E. Whittaker (1987). *A History of the Theories of Aether and Electricity*, Vols. I and II (American Institute of Physics, New York).
23. D. Pye (2001). *Polarised Light in Science and Nature* (Institute of Physics Publishing, Bristol, UK).

*Evgeniy Zubko, Mark Thoreson, Vsevolod Ivanov, Pavel Litvinov, Oleg Dubovik, Valery Loiko, Matthew Easley, Olga Kalashnikova, Rosario Vilaplana, Ben Veihelmann, James McDonald, Hal Maring, Karine Chamaillard, Michael Mishchenko, and Tracy Smith (from left to right). Photo courtesy Ivan Mishchenko.*